

Dear Editor,

Thank you for your work on our manuscript. Please find below details of the manuscript changes in response to the reviewer comments.

Best wishes,

Rachel Hawker.

Replies to review RC1

Review of Hawker et al. (2020): The nature of ice-nucleating particles affects the radiative properties of tropical convective cloud systems, submitted to Atmospheric Chemistry and Physics.

Thank you for your helpful comments on our paper. Note that as a result of additional figures in response to review RC2, the figure numbers in our responses to this review are different to those in the original manuscript.

General comments:

The authors present a very interesting study on the effect of different INP parametrizations on the radiative budget in Tropical Atlantic deep convective cloud fields. In particular, they show that INP parametrizations with a larger temperature-dependency lead to a larger increase in domain-mean daytime top of atmosphere outgoing radiation. In contrast to previous work by other authors, they present data that indicates primary ice production to be relevant also in presence of secondary ice formation. It should be clarified that the INP parameterizations tested against the Hallett-Mossop process explicitly, since this is the only SIP considered in the model.

Change to paper: We have made clearer in the text that the only SIP tested in this study was the Hallett Mossop process. We have also highlighted more explicitly that the results are only relevant to the Hallett Mossop process and future studies should explore the impact of INP in the presence of other secondary ice production mechanisms. We have detailed our changes below, but for example in the abstract, we now state *‘The controlling effect of the INP temperature dependence is substantial even in the presence of Hallett Mossop secondary ice production.....’*

The writing (from an editorial standpoint) is to be commended. The methodology appears stringent and valid with one minor aspect to be clarified. The work addresses relevant scientific atmospheric questions with impacts on global climate simulations. The title speaks of the nature of INPs, but the paper never refers back what “the nature” explicitly is. The topic of the paper is well suited for ACP. I recommend the manuscript for publication if the above and following comments below are addressed:

Change to paper: We have rephrased the title and any mention of the ‘nature of INP’ in the text to refer instead to the INP parameterisation choice or the temperature dependence of the INP number concentration.

Specific comments:

Line 19-20: The paper presented tests the effect of 5 parameterizations on radiation and SIPs but the word parameterization doesn’t shown up even once in the abstract. Also, the work is not explicitly testing the impact of the nature of the INPs (i.e. bio and physico-chemical properties of INPs). It is testing the impact of the various parameterizations which are based on desert dust, feldspar and continental aerosol, so there isn’t an explicit testing of physico-chemical properties of INP on the radiation. The C86 and M92 are not aerosol based either. I suggest being more explicit about what this work does. Same goes with the title, the nature of the INP is not tested as much as the type of parameterization.

Change to paper: The title has been changed to “The **temperature dependence** of ice-nucleating particle **concentrations** affects the radiative properties of tropical convective cloud systems” and the lines in question have been changed to “Our results show that the domain-mean daylight outgoing radiation varies by up to 18 W m⁻² depending on **the chosen INP parameterisation**. The key distinction between different INP **parameterisations** is the temperature dependence of ice formation, which alters the vertical distribution of cloud microphysical processes.”

Line 22: should add “due to the Hallett-Mossop process” after “...secondary ice production” since the paper tests the parameterizations against one secondary ice process, not all.

Change to paper: We have added ‘Hallett-Mossop’: ‘The controlling effect of the INP temperature dependence is substantial even in the presence of Hallett Mossop secondary ice production’

Line 51: Add Peckhaus et al. (2016) to the references who also studied different types of feldspars and reported ns.

Change to paper: As suggested.

line 53: Are e.g. mineral dust events not driven by meteorological factors (gust fronts, lack of precipitation, convective instability, trade winds, etc.) and have a major impact on INP concentrations?

Reply: The reviewer is correct that meteorological factors strongly influence dust concentrations in the Cape Verde region, but a number of studies have found that simple meteorological variables such as temperature and pressure are poor predictors of INP number concentrations.

Change to paper: We have edited this to read ‘Although INP concentrations do not simply correlate with meteorological variables such as pressure and temperature...’. We have also added (Price et al., 2018) to the citation which found large variability in INP number concentrations of ‘African continental’ INP filter samples during the ICE-D field campaign (see Figure 9 and the associated discussion in Section 3.1 of Price et al. (2018)).

Line 59-60: Not sure what the authors means here. Can this sentence be elaborated upon, or restructured?

Reply: The sentence in question highlighted that the studies in question did not alter the temperature dependence of the INP number concentration or used the same INP parameterisation in their approach.

Change to paper: The sentence has been changed to “However, in these model studies perturbations to INP number concentrations have predominantly involved uniform increases in aerosol or INP concentrations with all simulations using the same INP parameterisation (Carrió et al., 2007; Connolly et al., 2006; Deng et al., 2018; Ekman et al., 2007; Fan et al., 2010; Gibbons et al., 2018; van den Heever et al., 2006; Phillips et al., 2005), **i.e. the temperature dependence of INP number concentrations was not altered.**”

Page 6 (line 165). Maybe it would help the reader to also convert the smallest allowable size of ice to an idealized diameter of a sphere, e.g. (i.e. 10⁻¹⁸ kg or ~0.1 μm in diameter)

Change to paper: As suggested, we have added the approximate effective radius to the text: “The ice splinters produced by the representation of the Hallett Mossop process are the smallest allowable size of ice in the model (i.e. 10⁻¹⁸ kg, **volume radius ~0.11 μm**)”

Line 183: What errors would you expect from SOCRATES not responding to changes in ice crystal or snow number concentration, or any changes to rain or graupel species? An over- or underestimation in radiative processes? Also, how does the model then account for changes in ICNC due to heterogeneous freezing?

Reply: As the reviewer notes, the lack of consideration of ice and snow particle number by the SOCRATES radiation scheme is an important limitation of the results presented here. As such changes to ICNC due to heterogeneous freezing are not represented in the calculations, except through any corresponding changes in ice crystal water path. Due to the complex interactions between multiple hydrometeor types in these simulations, we don’t feel

able to give an accurate estimate of whether our results would under- or overestimate the radiative process. We acknowledge that the outgoing radiation simulated here may change with the inclusion of particle number and size from snow or ice, or from the inclusion of rain and graupel, and this is clearly stated and discussed in Section 4. The difference the inclusion of particle number from snow or ice would make to the outgoing radiation will vary across the domain and over time depending on whether the ‘real’ modelled effective radius was larger or smaller than the one implicitly assumed by the radiation code.

Line 189: If LW radiation is only calculated for daytime, how biased is this estimate, since LW would be most effective (trapping outgoing radiation) at night time, so how will this bias the results presented for outgoing LW radiation.

Reply: We decided to only calculate the radiative differences for the daytime hours because the simulation is 24 hours in length and includes 6 hours of spin up. Including the night-time hours in the radiation calculations would either mean including the spin up or averaging over 18 hours which gives an artificial dependence on simulation length (because we would be excluding some of the dark hours). Therefore we felt the most consistent and meaningful way to report the radiation differences was to analyze the daytime hours only. The inclusion of night-time values would reduce the contribution of shortwave to the total outgoing radiation differences shown in Figure 4a. The difference between including and excluding night-time values when averaging the outgoing longwave radiation was checked and found to be negligible.

Line 196: should “(ΔRad_{REFL})” come after the word “...difference” in the sentence? It seems to appear too early in the sentence.

Change to paper: The sentence has been changed as follows to make the definition of (ΔRad_{REFL}) clearer:

“The cloudy regions contribution, i.e. the difference in outgoing radiation between two cloudy regions due to changes in cloud albedo or thickness ignoring any changes in cloud fraction, (ΔRad_{REFL}) to a domain radiative difference....”

Line 197: What do s and r stand for? It is hard to follow the equations below without knowing some sort of physical definition of s and r.

Reply: s refers to a generic sensitivity simulation (e.g. a simulation using a specific INP parameterisation while r refers to a generic reference simulation (e.g. a simulation without any INP).

Change to paper: The following lines have been amended to make the use of s and r for the purposes of this paper clearer:

*“The cloudy regions contribution, i.e. the difference in outgoing radiation between two cloudy regions due to changes in cloud albedo or thickness ignoring any changes in cloud fraction, (ΔRad_{REFL}) to a domain radiative difference **between a sensitivity simulation (s) and a reference simulation (r) (s – r) is calculated using Eq. (1).***

$$\Delta Rad_{REFL} = cf_r \times \Delta Rad_{cl} \quad (1)$$

*where cf_r is the cloud fraction of simulation r and ΔRad_{cl} is the change in outgoing radiation from cloudy areas only between simulations (s – r). **The reference run (r) in Sections 3.1 – 3.4 refers to the NoINP simulation while the sensitivity run (s) are simulations which include an INP parameterisation. In Section 3.5, the reference run (r) refers to a simulation which has no representation of SIP and the sensitivity run (s) to a simulation which includes SIP due to the Hallett Mossop process.***”

Line 201: I am not sure if I followed equation 2 correctly, but could Δcf in this equation be replaced with ($Rads_{cl} - Rads_{cs}$) since you are looking at the contributions of cloud fraction to radiation between simulation s and r? If this is correctly understood, I would replace the Δcf with ($Rads_{cl} - Rads_{cs}$), to make it easier to follow equation 2. Or define Δcf more explicitly than has been done in line 203.

Reply: This equation calculates the change in outgoing radiation due to the increase or decrease in domain cloud fraction and as such calculates the change in outgoing radiation that occurs when an area in simulation s that was clear sky becomes cloudy in simulation r (or vice versa). It therefore calculates the average difference between cloud and clear sky in simulation s and multiplies this by the proportion of the domain that the change occurs in (the cloud fraction change between simulation s and r , or Δcf). This therefore assumes that the outgoing radiation from cloudy and clear regions in simulations s and r is the same. We know this assumption is false from the result of Equation 1 which is why we calculate the interaction effect (i.e. what the contribution of changes in cloud reflectivity or thickness in regions that have become cloudy is) to domain outgoing radiation from cloudy and clear sky regions in Equation 3. However the contribution of ΔRad_{INT} calculated in Equation 3 was negligible and therefore we are happy that Equation 2 captures the majority of the change in outgoing radiation due to cloud fraction change.

Change to paper: We have altered the description of Equation 2 as follows to make clearer what the equation defines and that Δcf refers to the change in domain cloud fraction between simulations s and r :

“The contribution of cloud fraction changes, i.e. the change in radiation that can be attributed to an area of clear sky in simulation s becoming cloudy in simulation r or vice versa, to the total change in domain outgoing radiation (ΔRad_{CF}) is calculated using Eq. (2).

$$\Delta Rad_{CF} = (Rad_{r,cl} - Rad_{r,cs}) \times \Delta cf \quad (2)$$

Where $Rad_{r,cl}$ is the mean outgoing radiation from cloudy regions in simulation r and $Rad_{r,cs}$ is the mean outgoing radiation from clear sky regions in simulation r and Δcf is the difference in **domain** cloud fraction between simulations s and r (s-r).”

Line 239: If the evolution of the clouds are not being discussed further, then no need to show the plots in figure 2e, f,g and h. The most useful plots are a-d since they compare the satellite with the model. Since there are no comparisons to the satellite for the other times, it doesn't give much of a validation. Also to show that the model produces a complex realistic cloud field can be demonstrated with Fig2c and 2d, so that c-h are not necessary.

Change to paper: As suggested.

Line 242: Same comment as above with Fig A2, panel c, d, e and f are not necessary.

Change to paper: As suggested.

Line 255: “flow” should be “flown”

Change to paper: As suggested.

Line 272: In the noINP case, can ice crystals that formed via homogeneous freezing, fall to lower levels and initiate secondary ice processes?

Reply: Yes, this is possible.

Change to paper: We have added the following sentence to clarify this:

“Ice crystals formed via homogeneous freezing can sediment to lower levels and initiate ice production via the Hallett Mossop process.”

Lines 281 to 283: similar to comment above, the comparison of noINP to simulations with INP parameterization demonstrates an enhancement in outgoing radiation for D10 and A13. Can the authors clarify here that noINP simulation excludes any contribution of SIPs that could result from ice settling from higher altitudes to warmer regions of the clouds? Or is such a contribution included in this assessment?

To me this seems possible to diagnose in the model, if the assessment of precipitation evaporating results in higher humidity such that the LWP due to increase cloud droplet number. Then why isn't the possibility of ice crystals or snow settling through the clouds at Hallett-Mossop relevant temperatures allowed to produce secondary ice?

Reply: The Hallett Mossop process can occur and produce ice due to ice settling in the NoINP simulation, as can be seen in Figure A4a.

Change to paper: We have added the bold sections in the following sentences to clarify this:

*"We first examine the effect of INP parameterisation on the outgoing radiation relative to the simulation where the only source of primary ice production was through homogeneous freezing (NoINP). **Cloud ice formed via homogeneous freezing can sediment to lower levels and initiate ice production via the Hallett Mossop process.** When contrasting the effect of different INP parameterisations in Sect 3.1-3.4, the Hallett Mossop process was always active **including in the NoINP simulation.** As stated in Sect. 2.1.3, the radiation code is represented by the Suite Of Community RAdiative Transfer codes based on Edwards and Slingo (SOCRATES) (Edwards and Slingo, 1996; Manners et al., 2017), and responds to changes in cloud droplet number and cloud droplet, ice crystal and snow mass. The results detailed below relate to either the domain-wide properties or all in-cloud regions within the domain. This means that the results describe the direct and indirect changes, **for example changes to the Hallett Mossop ice production, occurring due to the presence of INP across all cloud present in the domain, including low-level liquid clouds, mixed-phase clouds without a convective anvil and very deep convective clouds with an anvil.**"*

Line 285-286: "Radiative changes from the NoINP simulation to the inclusion of INP are caused mainly by .."

It is not clear to me what is meant by this statement. I think it means the difference in radiation between the NoINP and the INP simulations mostly arises from the changes in outgoing SW radiation, but if that is the case why not state it more simply, i.e. the difference in radiation between NoINP and INP simulations ...

Change to paper: As suggested.

Lines 291 – 292: The reported comparatively small change in TOA radiation when SIP is active relative to when it is inactive mentioned here, could this be because in the homogeneous freezing run SIP is by default assumed to be absent (i.e. settling of crystals to warmer Hallett-Mossop regions for secondary ice is not represented in the model)?

Reply: The settling of crystals to warmer Hallett-Mossop regions for secondary ice is represented in the model and is allowed to produce secondary ice as can be seen in Fig A4a.

Change to paper: We have added the bold in the following sentence to make this clear:

*"Bear in mind that SIP was active (SIP_active) in the simulations summarised in Fig. 4a, **including in the NoINP simulation in which the Hallett Mossop process can be initiated by settling ice crystals,** indicating that these cloud systems are sensitive to INP even in the presence of SIP."*

Line 293: The relationship between the slope of the parameterization and the outgoing radiation is implicit and not explicit. So stating that it is the key determinant seems very strong here, without clarifying that the slope is representative of the INP concentration as a function of T (Fig 1). It is the T at which a certain proportion of INPs are active is they key determinant and the physical reason for the strong influence on available supercooled liquid to be transported to higher altitudes of the MPC region. Could this relationship be clarified to invoke the temperature dependence rather than just stating the slope of the parameterization is the key determinant?

Reply: This comment is correct in that it is the INP concentration as a function of T that is important. We have termed this dependence of INP number concentration on temperature as the slope for simplicity as stated in the introduction "In particular, we examine the importance of the dependence of INP number concentration on temperature, referred to as INP parameterisation slope herein, as a major factor that determines cloud properties."

Change to paper: We have altered this line as follows to make clearer that it is the temperature dependent concentration that is important:

“The slope of the INP parameterisation (i.e. the dependence of INP number concentration on temperature) is a key determinant of the outgoing radiation.”

Line 303-304: This sounds counterintuitive to me because compared to the NoINP simulation, the increase in INP should increase the ICNC and decrease the cloud lifetime or outgoing SW (reflectivity) compared to otherwise what would be a more reflective liquid cloud with less ice. However further down the authors do explain why they observe this, because the liquid water path increases in the warmer part of the cloud which increases the outgoing SW. However, I find this assessment to be biased, without accounting for potential SIP in the NoINP simulation due to settling ice crystals.

Reply: We have addressed the issue of SIP in the noINP case above. To be clear, SIP due to settling ice crystals is possible in the NoINP simulation, as can be seen in Figure A4a. In the Hallett Mossop region, the ICNC is lowest in the NoINP simulation (see Figure AC1 below) because of the reduced production of ice by SIP. However, in all other regions of the cloud, including the upper mixed phase temperatures, ICNC is highest in the NoINP simulation due to the enhanced ice production by homogeneous freezing (Figure A4b), and subsequent settling of the ice crystals.

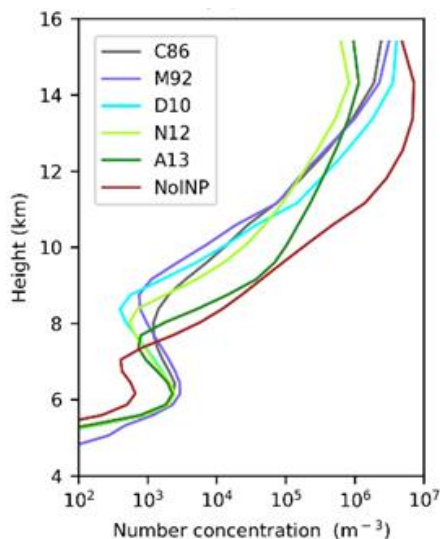


Figure AC1. In-cloud profile of ice crystal number concentration in the parameterisations that included SIP by the Hallett Mossop process.

Line 309/Figure 4b: I would have expected the water path due to snow to decrease because snow should leave the cloud faster than ice crystals? So why is the water path due to ice crystals decreasing? Or does it have to do with the categorisation of when a hydrometeor is considered a snow flake vs. an ice crystal in the model? Also, I would have expected that the increase in water path should be the lowest for the M92 and not for the D10, since the M92 has the shallowest slope?

Reply: The water path of ice crystals (cloud ice) decreases (in all except A13) when INP are included because in the NoINP simulation, more homogeneous freezing occurs and these ice crystals can settle through the cloud. In the simulations with INP, snow production is enhanced in the mixed-phase region (Figure A4c) due to enhanced accretion, riming and aggregation which increases the in-cloud snow water path. This increase is large enough to compensate for any decreases in snow mass that may occur due to increased settling. The changes in snow water path do not correspond to INP parameterisation slope because the increase in snow mass is relatively similar between all parameterisations (Figure A4c).

Lines 313-320: If the precipitation is increased, then the snow and graupel should not be part of the cloud anymore and thus not contribute to the increased reflected shortwave radiation. If the increased condensate is falling as precipitation such that it is resulting in an increased humidity thus increasing the LWP from an increase in cloud droplets, how can it

also contribute to increasing the outgoing shortwave in the cloud? It should either be classified as increased precipitation below cloud or increased condensate in-cloud leading to outgoing shortwave.

Reply: The in-cloud snow and graupel mass is enhanced significantly from the NoINP simulation (Fig A4c, d), allowing a proportion of snow and graupel to both remain 'in-cloud' and precipitate out of cloud to cause increased humidity at low cloud levels. Once the snow and graupel precipitate out of cloud below the melting temperature, they will be classified as rain in the model. Rain is excluded from the cloud mass threshold and thus hydrometeors that have precipitated out of cloud and melted are not included in the 'in-cloud' values.

Change to paper: We have added the bold text to the following sentence to clarify this:

*"At the same time, the enhanced production of relatively heavy snow and graupel increases precipitation which **on melting to form rain below the freezing level and subsequent** evaporation below 4 km, reduces out-of-cloud temperature and increases relative humidity (Fig. A5a, b)."*

Lines 321 – 334: This explanation makes more sense and sounds stronger and more convincing to me than the explanation in lines 308 to 320. Perhaps it would be better to shift the order of these paragraphs and explain the higher outgoing shortwave by the increased CDNC at lower altitudes due to increased LWP from lower freezing rates arising from steeper INP parameterizations (which imply very little het. freezing at small supercooling).

Reply: The lines in question relate to the difference in outgoing radiation from cloudy regions between simulations using different parameterisations and the impact of the temperature dependence of INP number concentrations. However, we feel it is logical and important to first address the reason for the change in outgoing radiation from the NoINP simulation before addressing the difference between different INP simulations.

Line 331: clarify statement more, I suggest (italics is suggested part) something like "...due to lower rates of heterogeneous freezing at the mid-bottom region of the mixed-phase cloud (lower supercooling, Fig. 1) and SIP at ..."

Change to paper: As suggested.

Line 339: clarify by inserting "cloud fraction due to" i.e. sentence should read

"...offset somewhat by decreases in the cloud fraction due to homogeneous freezing in the ~10 – 14 km regime (Fig 6a)"

Change to paper: The sentence has been altered as suggested with one minor difference: "offset somewhat by decreases in the cloud fraction due to **reduced** homogeneous freezing in the ~ 10 - 14 km regime (Fig. 7a)"

Line 358-360: If this is true, (and it sounds like a good explanation), shouldn't the decrease in outgoing LW shown in Figure 4a be the highest for A13 and not for C86. Because A13 results in the highest number of ICNC at the top of the MPC region and in the homogeneous freezing region therefore should trap most of the outgoing LW radiation thus giving the most decrease in the outgoing LW.

Reply: The sentence in question refers to the ratio of ice crystals to snow and graupel which affects the cloud fraction, not their absolute values which effects the cloud thickness and thus the outgoing longwave. The decrease in outgoing longwave radiation would be greatest for A13 if the only thing contributing to outgoing longwave was ice crystal number or ice crystal mass, however the change in outgoing longwave from cloudy regions is due to changes in all of snow, ice crystals and cloud droplets. The decreases in longwave are predominately due to increases in total waterpath, and thus cloud thickness, from cloud droplets, ice crystals and snow particles. C86 has the greatest combined water path from cloud droplets, ice crystals and snow particles (Figure 4c) and thus the largest decrease in outgoing longwave from the NoINP simulation.

Line 379: Change to "It has been argued that the observed (or derived) primary ice particle production rate...". Otherwise, the statement is false, because if the primary production rate is high, the secondary ice production (H-M process) would be low but still present, primary ice production would in fact dominate cloud properties.

Change to paper: As suggested.

Line 384/ line 219/lines 440-445: Most relevant comment. You show that higher primary ice production rates in the temperature range between 253 and 238 K, e.g. in A13, have a large impact on the total on top of atmosphere outgoing radiation, yet you exclude SIP which are active at colder temperatures than 265 K. Can you elaborate on the expected impact/uncertainty in your results and concluding statement, (SIP is less important than primary ice production) stemming from your simplification that SIP is only including Hallett Mossop process? Please justify why your concluding statement is valid.

Reply: It is correct that we have only modelled Hallett Mossop SIP and have made this much clearer in the revised paper (i.e. rather than referring generally to SIP, we refer to Hallett-Mossop SIP). However, it is also true that other theoretical SIP mechanisms are unquantified and it has not been clearly shown that they need to be included in models, beyond specific cases. As understanding of other potential SIP mechanisms emerges they should be included and assessed in studies like this one in future research.

Change to paper: We have clarified wherever relevant that the only SIP included in our simulations is the Hallett Mossop process and caveated if necessary that the results may be different if other mechanisms of SIP were included.

Line 383-384: This is an important outcome of the study, but should be caveated with the notion that other possible known and unknown SIPs are not considered. The authors in part do that by acknowledging in parenthesis that the SIP considered is the H-M, but I think they could go one step further in saying that this could change with more parameterizations and quantification becoming available for lower temperatures where SIP becomes important say below 265 K (Lauber et al., 2018).

Change to paper: As suggested.

Page 14 (line 385). An average impact comparison in the text might be supportive for the reader (e.g. mean over all parameterizations total INP impact 9.8 W/m² to total SIP impact 2.7 W/m²)

Change to paper: As suggested.

Line 453-455: A possible explanation for this statement should be given here in in the conclusions, since this is an important point or outcome of the study. Have the other studies that are mentioned in these lines also only tested the influence of the Hallett-Mossop process? If not, this should be clarified. Further, since this has evaluated the influence of SIP due to the HM process, it should be stated here in the conclusions.

So this conclusion is true, when the SIP being considered is HM. But it remains open if the conclusions would still hold if freeze shattering and other mechanisms (e.g., as described in Lauber et al., 2018) were included in the models.

Reply: The papers cited either explicitly tested the Hallett Mossop process or inferred using observational data that INP concentrations were relevant up to a threshold needed to initiate the Hallett Mossop process.

Change to paper: The section has been modified to make clear that only the Hallett Mossop process was included.

Line 496: In addition to Holden et al. (2019) the authors could add Coluzza et al. (2017) and Kanji et al. (2017) since that lack of knowledge on what constitutes the identity of an active site was already discussed in these publications.

Change to paper: As suggested.

Line 497: The last statement here has surely been mentioned before by other authors in numerous publications. While it is valuable that the authors also come to this conclusion (need for INP measurement across the entirety of the MPC regime), this study is not the first to recommend such an outlook and the sentence can be modified to say “.as reported before by XX..”

Change to paper: As suggested the line in question has been altered to “This work demonstrates the importance of solving these problems and measuring INP number concentrations across the entirety of the mixed-phase temperature spectrum, **as has been demonstrated in previous work (e.g. Liu et al., 2018; Takeishi and Storelvmo, 2018).**”

Figure 2: Should there not be a "radiation" in the color bar caption, e.g. Outgoing OA longwave radiation (W m⁻²)?

Change to paper: As suggested. The same change was made in Figure A1.

Figure 5: Colour legend is missing. I suggest adding it here even if it is the same as previous figures for ease of reading.

Change to paper: As suggested.

Appendix A, page 34 (Figure A1). The three kind of blue lines are not easy to distinguish from the black line.

Change to paper: The blue lines in the plot in question (Now Figure 1b,c) have been changed to red.

Appendix A, page 34 (Figure A1). What does the unit of / 10⁸ m⁻³ mean? Is it two particles per 10⁸ m⁻³ of volume?

Change to paper: Changed to ‘10⁸ m⁻³’ to reflect 10⁸ particles m⁻³ of volume (now Figure 1b). There was a similar error in Figure 7b y-axis units changed from /10⁻⁵ m⁻³ to ‘10⁵ m⁻³’.

Figure A3 panel a: what are the regions filled with black colour? Could the colors be changed so that the contrast between green and blue is better visible? If black is just the border of the bars, I suggest removing the borders since it reduces clarity of the plot suggesting that there is a third colour.

Change to paper: As suggested, the black outline has been removed.

Line 810: Histograms should be singular not plural.

Change to paper: As suggested.

References

Coluzza, I., Creamean, J., Rossi, J. M., Wex, H., Alpert, A. P., Bianco, V., Boose, Y., Dellago, C., Felgitsch, L., Fröhlich-Nowoisky, J., Herrmann, H., Jungblut, S., Kanji, A. Z., Menzl, G., Moffett, B., Moritz, C., Mutzel, A., Pöschl, U., Schauperl, M., Scheel, J., Stopelli, E., Stratmann, F., Grothe, H., and Schmale, G. D.: Perspectives on the Future of Ice Nucleation Research: Research Needs and Unanswered Questions Identified from Two International Workshops, 8, doi:10.3390/atmos8080138, 2017.

Holden, M. A., Whale, T. F., Tarn, M. D., O’Sullivan, D., Walshaw, R. D., Murray, B. J., Meldrum, F. C., and Christenson, H. K.: High-speed imaging of ice nucleation in water proves the existence of active sites, 5, eaav4316, doi:10.1126/sciadv.aav4316, 2019.

Kanji, Z. A., Ladino, L. A., Wex, H., Boose, Y., Burkert-Kohn, M., Cziczo, D. J., and Krämer, M.: Overview of Ice Nucleating Particles, in: Ice Formation and Evolution in Clouds and Precipitation: Measurement and Modeling Challenges, 2017.

Lauber, A., Kiselev, A., Pander, T., Handmann, P., and Leisner, T.: Secondary Ice Formation during Freezing of Levitated Droplets, 75, 2815-2826, doi:10.1175/JAS-D-18-0052.1, 2018.

Peckhaus, A., Kiselev, A., Hiron, T., Ebert, M., and Leisner, T.: A comparative study of K-rich and Na/Ca-rich feldspar ice-nucleating particles in a nanoliter droplet freezing assay, Atmos. Chem. Phys., 16, 11477-11496, doi:10.5194/acp-16-11477-2016, 2016.

Replies to review RC2

Review “The nature of ice-nucleating particles affects the radiative properties of tropical convective cloud systems” by R. E. Hawker, et al.

Thank you for your constructive comments on our paper.

This modeling study investigates the effects of ice nucleating particles (INP) on the radiative properties of tropical convective cloud system. Several widely used INP parameterizations are used in the model, and interestingly the slope of the INP temperature dependence is found to play a key role in the INP effects. The effects of secondary ice production (SIP) are studied, which demonstrate the important role of INP nature for the SIP effects. The study examines the difference aspects of cloud microphysical properties and cloud fraction to understand the INP effects on radiative forcing. Generally, the research topics of INP and SIP and effects on convection are interesting and the results are novel. The manuscript may be accepted for publication after addressing my comments.

Main comments

1. Adding a schematic to illustrate how different slopes of INP temperature dependence could affect cloud microphysics at different vertical layers of convective clouds. That will help readers to better understand the interactions.

Change to paper: As suggested, a schematic has been added (Fig. 9, shown below)

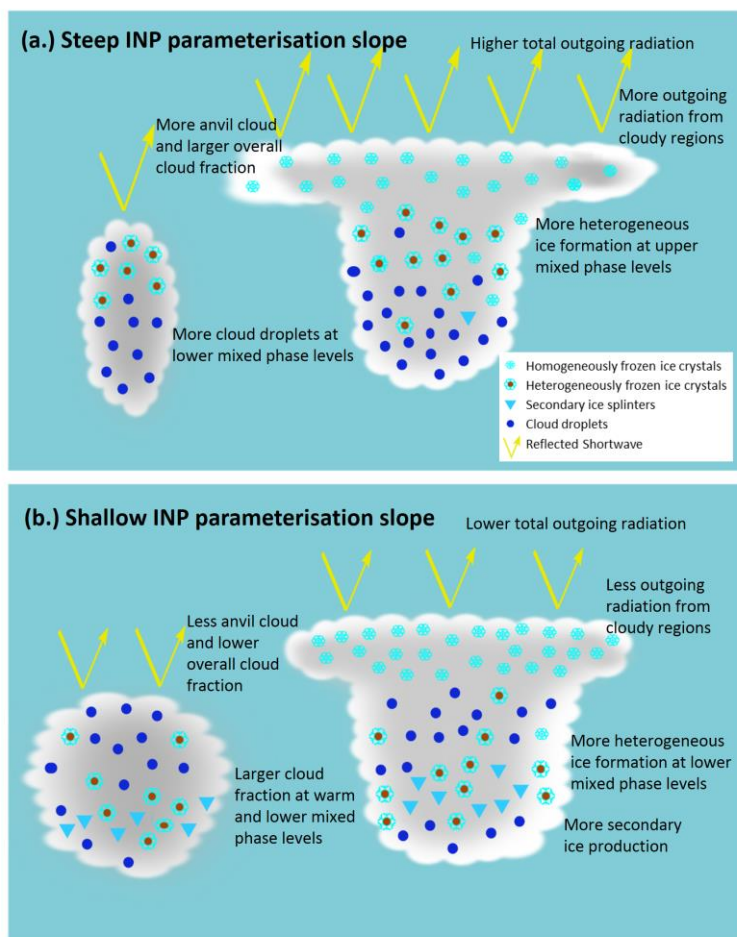


Figure 9. Schematic of the main effects of INP parameterisation slope (i.e. a steep (a) or shallow (b) temperature dependence of INP number concentrations).

2. A better description of model configuration such as model domain, and initial thermodynamical profiles, is required.

Change to paper: As suggested. Fig. 1a (shown below) has been added to the paper to better illustrate the domain location and how the global model is used to initiate the nested domain. Fig. A1a and b (now Fig. 1b, c, shown below) have been moved to the main paper so that the initial aerosol profiles are clearer to the reader. More detail has been added to the reference to the global model (from “The Met Office global model is used to initialise the nested simulation” to “A global model simulation (UM vn 8.5, GA6 configuration, N512 resolution (Walters et al., 2017)) is used to initialise the nested simulation”).

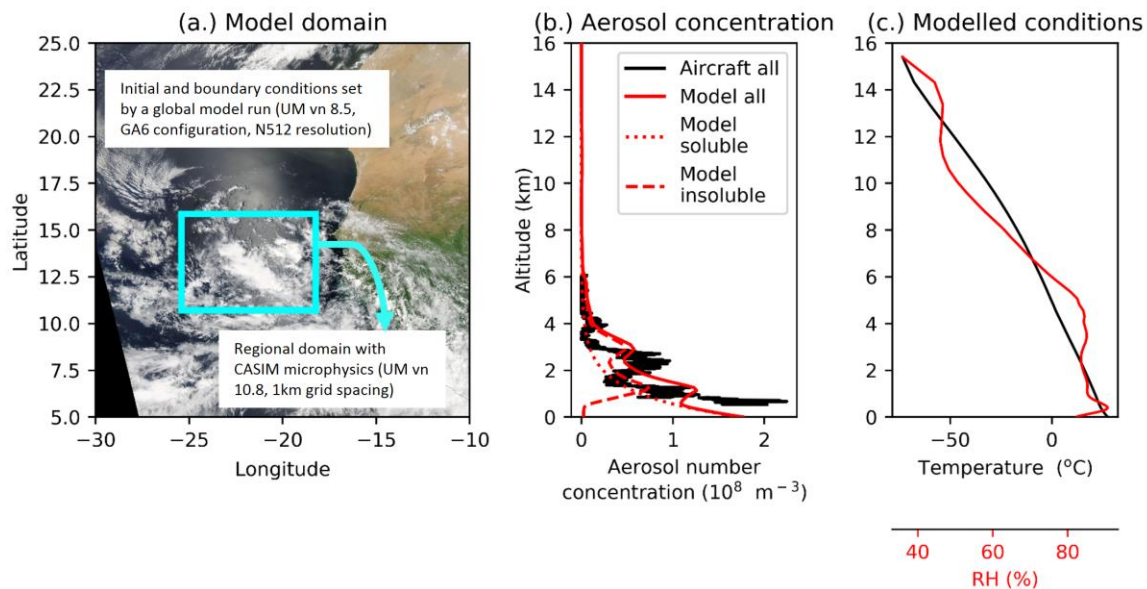


Figure 1. Modelled domain location and resolution details (a), observed (black line) and modelled (red lines) aerosol concentrations (b), and mean modelled domain mean temperature and relative humidity profiles (c). The observed aerosol profile shown in b was measured using the Passive Cavity Aerosol Spectrometer Probe (PCASP) which captures aerosols between 0.1 and 3 μ m in size. The insoluble aerosol profile shown in b is extracted from a regional UM vn 10.3 simulation (8 km grid spacing, CLASSIC dust scheme). The modelled aerosol profiles are applied throughout the regional domain shown in a at the start of the simulation (00:00 21st August 2015) and at the boundaries throughout. INP concentrations in the D10, N12 and A13 simulations are linked to the insoluble aerosol profile shown in b. The image shown in (a) are moderate resolution imaging spectroradiometer (MODIS) Corrected Reflectance imagery produced using the MODIS Level 1B data and downloaded from the NASA Worldview website.

Change to paper: As a result of the above two changes the numbers of the other figures in the paper have been changed.

Minor comments

1. Line 45: “..INP number concentrations can vary by as much as six orders of magnitude at any one temperature”. Can you add some reasons to explain this large variability?

Change to paper: The sentence in question has been altered to

“Measurements indicate that INP number concentrations can vary by as much as six orders of magnitude at any one temperature due to variations in, for example, aerosol source, chemical or biological composition and surface morphology (DeMott et al., 2010; Kanji et al., 2017).

2. Line 56: “...global models based on known INP-active materials show reasonable skill in simulating global INP concentrations (Vergara-Temprado et al., 2017).” There are also other studies that can be cited here: e.g., Shi and Liu (2019), GRL, compared the modeled INPs with observations.

Change to paper: As suggested

3. Line 81: “and droplets can freeze homogeneously below around -33°C ”. Does your model represent the homogeneous freezing of aerosol droplets below around -37°C ?

No, it represents the freezing of cloud droplets only.

4. Lines 93-103. You can add one sentence here to introduce your work on SIP effects and dependence on INP parameterizations.

Change to paper: As suggested.

5. Section 2.1.1. Please add a figure in main text showing the model domains and how different models, cloud microphysics, and aerosols are applied to these domains.

Change to paper: As suggested, a new figure has been added showing the model domains. Former Fig. A1a and b was combined with this new figure becoming Fig. 1b and c.

6. Line 131. “five hydrometeor classes (cloud droplets, rain droplets, ice crystals, graupel, snow)”. It would be clearer to use “cloud ice” to replace “ice crystals” since ice crystals can contain snow and graupel particles. Also changes the words in text.

Change to paper: We have clarified in this sentence that throughout the paper ice crystals refers to cloud ice.

7. Line 149. You can make it clear the insoluble aerosol is dust which is used in N12 and A13 parameterizations.

Change to paper: We have altered “insoluble aerosol” to “insoluble **dust** aerosol”.

8. Line 158: “predict an ice production rate via heterogeneous freezing”. These ice nucleation parameterizations (M92, N12, D10) only predict INP number concentrations. How do you calculate the ice production rate?

Reply: CASIM examines the gridbox temperature, cloud number, ice number and, in the case of D10, N12 and A13, the insoluble aerosol concentrations. If the cloud number is above a minimum threshold and the temperature is below 0°C , it calculates the available INP. It then subtracts the existing ICNC in the gridbox from this calculated INP number concentration to calculate the ice crystals produced by heterogeneous freezing giving an ice production rate. The number of ice crystals produced by heterogeneous freezing is output as a 3D diagnostic from the model.

Change to paper: We have altered the sentence as follows to make it clearer what else other than insoluble aerosol number concentration is used to calculate the rate of ice production.

*“The INP parameterisations inspect the conditions (**temperature, cloud droplet number, ICNC**) and aerosol concentrations within a gridbox and use that information to predict an ice production rate via heterogeneous freezing.”*

9. Line 159. Do you also represent the CCN wet scavenging?

Reply: No the aerosols are not depleted by cloud droplet activation or ice nucleation in these simulations. We have clarified this in the second paragraph of Section 2.1.2.

10. Line 223. It would be good to note that these INP parameterizations only applied to certain temperature ranges and cannot reliably extrapolate to temperatures outside the range.

Change to paper: As suggested, we have added the following to make this clear:

“It should be noted that all parameterisations tested in this work were developed between specific temperature ranges and extrapolation beyond these temperatures adds uncertainty. However, for the purposes of this paper and to allow a direct comparison between parameterisations, all parameterisations have been applied between 0 and -37°C .”

11. Section 3.5. Line 384. How do other SIP mechanisms impact your results here in this section?

Reply: Other SIP mechanisms are not included in the model simulations. Their inclusion may alter the results presented which only relate to the Hallett Mossop process because it is the most well-known and best quantified SIP mechanism.

Change to paper: The paragraph in question has been altered as follows to highlight the limitations and caveats of not including other SIP mechanisms:

*“We find that the microphysical and radiative properties of the cloud field depend strongly on the properties of the INP even **when SIP due to the Hallett-Mossop process occurs**. Furthermore, the effect of including SIP on daylight domain-mean outgoing radiation varies between -2.0 W m^{-2} and $+6.6 \text{ W m}^{-2}$ (Fig. 4b), showing that **the presence of the Hallett Mossop process** has a smaller effect than the INP parameterisation **and that the sign and magnitude of this effect depends on the INP parameterisation**. Therefore, rather than primary ice being simply overwhelmed by SIP, it actually determines how SIP affects cloud microphysics. **Other mechanisms of SIP have been proposed (Field et al., 2017; Lauber et al., 2018) and the impact of INP on cloud properties in the presence of these mechanisms, particularly those present at temperatures below 10°C such as droplet shattering (Lauber et al., 2018), should be tested in future but this was beyond the scope of the present study.**”*

12. Line 399-407. As commented above, a schematic showing the interactions and mechanisms would be helpful for the readers.

Change to paper: As suggested, a schematic has been added to the paper (Fig. 9)

13. Line 412. Since CASIM is a two-moment cloud microphysics scheme, why are ice and snow particle numbers not used in the radiation scheme?

Reply: The SOCRATES radiation scheme is the radiation component of the Met Office Unified Model, and has not yet been fully coupled to the CASIM microphysics module. As such ice and snow particle numbers, and thus size, have not yet been included in the radiation calculations. The incorporation of ice and snow particle numbers into the SOCRATES scheme is a desirable feature for future model development but was beyond the scope of this paper.

14. Line 415. It is not correct to state: “climate models do not typically represent ICNCs”. Please remove.

Change to paper: Altered as follows to be more specific that we are referring only to the representation of ICNC in radiation calculations in climate models:

*“However, our results are still very relevant for climate model simulations as **climate models typically employ single moment microphysics schemes that do not explicitly predict ICNC for the purposes of inclusion in radiation calculations and have frequently been shown to poorly represent ice crystal mass concentrations (Baran et al., 2014b; Waliser et al., 2009).**”*

The ~~nature~~ temperature dependence of ice-nucleating particle concentrations affects the radiative properties of tropical convective cloud systems

Rachel E. Hawker^{*1}, Annette K. Miltenberger^{1, a}, Jonathan M. Wilkinson², Adrian A. Hill², Ben J. Shipway², Zhiqiang Cui¹, Richard J. Cotton², Ken S. Carslaw¹, Paul R. Field^{1, 2}, Benjamin J. Murray¹.

1. Institute for Climate and Atmospheric Science, University of Leeds, Leeds, LS2 9JT, United Kingdom.

2. Met Office, Exeter, EX1 3PB, United Kingdom.

a. now at : Institute for Atmospheric Physics, Johannes Gutenberg University Mainz, Mainz, 55128, Germany.

Correspondence to: Rachel E. Hawker (eereh@leeds.ac.uk)

Abstract

Convective cloud systems in the maritime tropics play a critical role in global climate, but accurately representing aerosol interactions within these clouds persists as a major challenge for weather and climate modelling. We quantify the effect of ice-nucleating particles (INP) on the radiative properties of a complex Tropical Atlantic deep convective cloud field using a regional model with an advanced double-moment microphysics scheme. Our results show that the domain-mean daylight outgoing radiation varies by up to 18 W m^{-2} depending on the chosen INP parameterisation ~~the bio- and physico-chemical properties of INP~~. The key distinction between different INP parameterisations is the temperature dependence of ice formation, which alters the vertical distribution of cloud microphysical processes. The controlling effect of the INP temperature dependence is substantial even in the presence of [Hallett Mossop](#) secondary ice production, ~~due to the Hallett Mossop process~~, and the effects of secondary ice formation depend strongly on the ~~nature of the INP~~ chosen INP parameterisation. Our results have implications for climate model simulations of tropical clouds and radiation, which currently do not consider a link between INP particle type and ice water content. The results also provide a challenge to the INP measurement community, since we demonstrate that INP concentration measurements are required over the full mixed-phase temperature regime, which covers around 10 orders of magnitude in INP concentration.

1. Introduction

Deep convective clouds are important drivers of local, regional and global climate and weather (Arakawa, 2004; Lohmann et al., 2016). They produce substantial precipitation (Arakawa, 2004) and the associated phase changes release latent heat that helps to drive global atmospheric circulation (Fan et al., 2012). Convective clouds have a direct impact on climate through interactions with incoming shortwave and outgoing longwave radiation (Lohmann et al., 2016), for example by producing radiatively important long-lived cirrus clouds (Luo and Rossow, 2004). The clouds extend from the warmer lower levels of the atmosphere where only liquid exists to the top of the troposphere where only ice exists (Lohmann et al., 2016). Between these levels is the mixed-phase region where both liquid and ice coexist and interact (Seinfeld and Spyros, 2006). Within the mixed-phase region, primary ice particles can form heterogeneously through the freezing of cloud droplets by ice-nucleating particles (INP). The importance and relative contribution of heterogeneous freezing to ice crystal number concentrations (ICNC) and resultant cloud properties, such as cloud reflectivity, is very uncertain (Cantrell and Heymsfield, 2005; Kanji et al., 2017). This uncertainty stems from the difficulty of predicting INP number concentrations (Kanji et al., 2017; Lacher et al., 2018) as well as the difficulty of quantifying complex interactions between heterogeneous freezing and other ice production mechanisms (Crawford et al., 2012; Huang et al., 2017; Phillips et al., 2005).

Understanding the effects of INP on convective clouds presents substantial challenges. Measurements indicate that INP number concentrations can vary by as much as six orders of magnitude at any one temperature due to variations in, for example, aerosol source, chemical or biological composition and, surface morphology (DeMott et al., 2010; Kanji et al., 2017), ~~and~~. Large variability exists even in measurements of individual regions or aerosol populations (Boose et al., 2016b; Kanji et al., 2017; Lacher et al., 2018). For example, there are four orders of magnitude variation in summertime measurements of INP number concentrations in the Saharan Air Layer at -33°C (Boose et al., 2016b). Even for particles of similar and known mineralogy, measurements of ice-nucleation efficiency can span several orders of magnitude: The spread in laboratory measurements of ice nucleation active site densities (n_s) for different types of feldspar spans seven orders of magnitude at -15°C (Atkinson et al., 2013; Harrison et al., 2016, 2019; Peckhaus et al., 2016). Our ability to understand and quantify such variability in INP concentrations has improved as more measurements have been made. Although ~~meteorological factors are not strong indicators of~~ INP concentrations do not simply correlate with meteorological variables such as pressure and temperature (Boose et al., 2016a; Lacher et al., 2018; Price et al., 2018), aerosol surface area (Lacher et al., 2018) and diameter (DeMott et al., 2015) provide

58 some predictability and global models based on known INP-active materials show reasonable skill in simulating global
59 INP concentrations (Shi and Liu, 2019; Vergara-Temprado et al., 2017).

60 It is known from model simulations that changes in INP number concentration affect the microphysical properties and
61 behaviour of deep convective clouds (Deng et al., 2018; Fan et al., 2010a, 2010b; Gibbons et al., 2018; Takeishi and
62 Storelvmo, 2018). However, in these model studies perturbations to INP number concentrations have predominantly
63 involved uniform increases in aerosol or INP concentrations with all simulations using the same INP parameterisation
64 (Carrió et al., 2007; Connolly et al., 2006; Deng et al., 2018; Ekman et al., 2007; Fan et al., 2010a; Gibbons et al., 2018;
65 van den Heever et al., 2006; Phillips et al., 2005), i.e. the temperature dependence of INP number concentrations has
66 not been was not altered. Where different INP parameterisations have been used (Eidhammer et al., 2009; Fan et al.,
67 2010b; Liu et al., 2018; Takeishi and Storelvmo, 2018), the results have in most cases been interpreted in terms of the
68 overall increase in INP number concentration (Fan et al., 2010b; Liu et al., 2018; Takeishi and Storelvmo, 2018).

69 However, there are important structural differences between different INP parameterisations that have not yet been
70 explored in detail. For example, currently available and regularly used parameterisations of INP vary substantially in
71 the dependence of INP activity on temperature. We hypothesise that the difference between parameterisations will
72 be particularly important for deep convective clouds because heterogeneous ice formation occurs over a very wide
73 temperature range from just below 0 to around -38°C in the mixed-phase region of these clouds. For the same dust
74 particle concentration, predicted INP concentrations can increase by up to three orders of magnitude from -15 to -
75 20°C (corresponding to approximately 1 km altitude change) using an INP parameterisation with a steep temperature
76 dependence (lower INP concentrations at high temperatures and higher INP concentrations at low temperatures)
77 (Atkinson et al., 2013), but by less than one order of magnitude using an INP parameterisation with a shallower
78 dependence (DeMott et al., 2010; Meyers et al., 1992). We hypothesise that such large differences in ice production
79 rates between INP parameterisations are likely to affect cloud properties. In simulations of deep convective clouds
80 over North America (Takeishi and Storelvmo, 2018) there were differences in the magnitude and altitude of droplet
81 depletion depending on INP parameterisation choice (Bigg, 1953; DeMott et al., 2010, 2015).

82 Uncertainty in mixed-phase cloud properties is compounded further by a lack of quantification of the interaction of
83 heterogeneous freezing with other ice production mechanisms. Ice crystals in the mixed-phase region can also be
84 formed by secondary ice production (SIP) from existing hydrometeors (Field et al., 2017) and droplets can freeze
85 homogeneously below around -33°C (Herbert et al., 2015). In observations of convective clouds with relatively warm
86 cloud-top temperatures (Fridlind et al., 2007; Heymsfield and Willis, 2014; Ladino et al., 2017; Lasher-Trapp et al.,

87 2016; Lawson et al., 2015), ICNC has frequently exceeded INP number concentrations by several orders of magnitude,
88 suggesting that secondary ice production is the dominant small-ice formation mechanism in mixed-phase regions
89 (Ladino et al., 2017). The importance of heterogeneous ice production relative to secondary and homogeneous
90 freezing has therefore been questioned (Ladino et al., 2017; Phillips et al., 2007) and it has been proposed that INP
91 concentrations may only be relevant up to a threshold needed to initiate SIP (Ladino et al., 2017; Phillips et al., 2007),
92 a value that may be as low as 0.01 L^{-1} (Crawford et al., 2012; Huang et al., 2017) for the Hallett Mossop process
93 (Hallett and Mossop, 1974). If this is the case, in clouds where SIP may also be initiated by the primary freezing of a
94 few large ($\sim 1 \text{ mm}$) droplets in a rising parcel (Field et al., 2017), INP number concentrations may be largely irrelevant
95 to cloud ice properties. The effect of INP and INP parameterisation on convective cloud properties must therefore be
96 examined with consideration for the presence of, and interactions with, SIP.

97 Here we explore how the choice of INP parameterisation affects the properties of a large and realistic cloud field
98 containing clouds at all levels as well as deep convective systems in the eastern Tropical Atlantic with a focus on the
99 top of atmosphere (TOA) outgoing radiation. The eastern Tropical Atlantic is an ideal location in which to examine the
100 role of INP concentrations in convective cloud systems because, owing to its position at the interface between the
101 Saharan Air Layer and the Inter Tropical Convergence Zone, it is subject to both high levels of convective activity and
102 high loadings of desert dust, a relatively well-defined INP type (DeMott et al., 2003; Niemand et al., 2012; Price et al.,
103 2018). First, we determine how the presence of INP alters the radiative properties of the cloud field. We then
104 examine how the properties of the simulated cloud field, including cloud shortwave reflectivity, cloud fraction and
105 anvil extent, depend on the choice of INP parameterisation. In particular, we examine the importance of the
106 dependence of INP number concentration on temperature, referred to as INP parameterisation slope herein, as a
107 major factor that determines cloud properties. We also examine the effect on cloud properties of the inclusion of SIP
108 due to the Hallett Mossop process.

109

2. Methods

2.1. Model set-up

2.1.1 Regional domain and initial conditions

Simulations described in this article were performed using the Unified Model (UM) version 10.8 (GA6 configuration) (Walters et al., 2017). The UM is a numerical weather prediction model developed by the UK Met Office. We use a regional nest within the global model simulation (Fig. 1a), which has a grid spacing of 1 km (900*700 grid points) and 70 vertical levels. Meteorology of the driving global model is based on operational analysis data. Within the nested domain, the Cloud AeroSol Interacting Microphysics scheme (CASIM) is employed to handle cloud microphysical properties. ~~The Met Office global model~~ A global model simulation (UM vn 8.5, GA6 configuration, N512 resolution (Walters et al., 2017)) is used to initialise the nested simulation at 00:00 on the 21st of August 2015 and is used throughout the simulation for the boundary conditions.

The 21st of August 2015 was chosen for simulation to coincide with flight b933 of the Ice in Clouds Experiment – Dust (ICE-D) July-August 2015 field campaign that targeted convective clouds extending to and beyond the freezing level. The aerosol profile measured during flight b933 (Fig. A1a1b) was used to derive the aerosol profiles prescribed over the nested domain at the beginning of the simulation and are constantly applied at the boundaries. Model profiles were calculated as follows: The UM vn 10.3 was used to simulate a domain comprising the entire Tropical Atlantic and West Africa. This simulation was initiated on the 18th August 2015 with a grid spacing of 8 km using the UM operational one-moment microphysics (i.e. not CASIM) and the CLASSIC aerosol scheme with a 6-bin dust model (Johnson et al., 2015a). On the day of the b933 flight (21st August 2015), a dust layer was present between 2 and 3 km altitude. Comparison to MODIS AOD data indicates agreement between the model and observations (not shown). This UM vn 10.3 simulation was used to calculate the average dust profile (mass and number concentration) over the CASIM domain on the 21st of August 2015 and these dust profiles are applied in the nested domain as the insoluble aerosol profiles (Fig. A1a1b). The approximate difference between the dust aerosol profile provided by the UM regional simulation and the observed aerosol profile measured during flight b933 (comprising both insoluble and soluble particles) is used as the soluble aerosol profile (Fig. A1a1b). The simulations are 24 hours in length.

2.1.2. CASIM microphysics

CASIM is a multi-moment bulk scheme, which is configured to be two-moment in this work. Both number concentration and mass concentration for each of the five hydrometeor classes (cloud droplets, rain droplets, ice

138 crystals (or cloud ice), graupel, snow) are prognostic variables. The model set-up is very similar to that used in
139 Miltenberger et al. (2018) including the parameter choices within CASIM. CASIM has been used and tested previously
140 in simulations of coastal mixed-phase convective clouds (Miltenberger et al., 2018), South-East Pacific stratocumulus
141 clouds (Grosvenor et al., 2017), Southern Ocean supercooled shallow cumulus (Vergara-Temprado et al., 2018),
142 midlatitude cyclones (McCoy et al., 2018) and CCN-limited Arctic clouds (Stevens et al., 2018).

143 Cloud droplet activation is parameterised according to (Abdul-Razzak and Ghan, 2000). The soluble accumulation
144 mode aerosol profile shown in Fig. ~~A1a~~1b is used for cloud droplet activation and a simplistic CCN activation
145 parameterisation is included for the insoluble aerosol mode (Abdul-Razzak and Ghan, 2000) that assumes a 5% soluble
146 fraction on dust. Scavenging of CCN or INP is not represented. Collision-coalescence, riming of ice crystals to graupel
147 and aggregation of ice crystals to snow is represented. Rain drop freezing is described using the parameterisation of
148 Bigg (1953). For reference, the modelled domain-mean out-of-cloud temperature and relative humidity are shown in
149 Fig. ~~A1c~~b. The model time-step is 5 seconds.

150 Heterogeneous ice nucleation is represented using 5 different parameterisations: Cooper (1986) (C86), Meyers et al.
151 (1992) (M92), DeMott et al. (2010b) (D10), Niemand et al. (2012) (N12) and Atkinson et al. (2013) (A13) (~~Fig. 4~~Fig. 2).
152 C86 and M92 calculate a freezing rate based on temperature and are independent of aerosol concentration. D10
153 calculates an INP concentration from temperature and the concentration of insoluble dust aerosol with a diameter
154 greater than 0.5 μm . N12 and A13 calculate an INP concentration from the temperature dependent active surface site
155 density and the surface area of insoluble dust aerosol (n_s). For A13, a potassium-feldspar fraction of 0.25 is assumed.
156 This is the upper recommended fraction (Atkinson et al., 2013) which was deemed appropriate because of the study
157 region's exposure to Saharan dust outflow. M92 is described as a deposition and condensation freezing
158 parameterisation (Meyers et al., 1992) and is often used alongside an immersion freezing parameterisation in
159 modelling studies (Deng et al., 2018; Fan et al., 2010b, 2010a; Gibbons et al., 2018). However, the M92
160 parameterisation is based on aircraft continuous flow diffusion chamber measurements and those measurements
161 should capture all relevant nucleation mechanisms (see Vali et al., 2015). To represent nucleation at conditions
162 relevant for clouds with liquid water present, we have set the saturation term in the M92 parameterisation to water
163 saturation. One simulation is conducted with no active heterogeneous ice nucleation representation (NoINP). The INP
164 parameterisations inspect the conditions (temperature, cloud droplet number, ICNC) and aerosol concentrations
165 within a gridbox and use that information to predict an ice production rate via heterogeneous freezing. The

166 supercooled droplets are depleted by the freezing parameterisation, but scavenging of INPs is not represented.
167 Homogeneous freezing of cloud droplets is parameterised according to Jeffery and Austin (1997).
168 Secondary ice production (SIP) is represented using an approximation of the Hallett Mossop process which occurs
169 between -2.5 and -7.5°C. The efficiency of the Hallett Mossop process increases from -2.5 and -7.5°C to 100% at -5°C.
170 The rate of splinter production per rimed mass is prescribed with 350 new ice splinters produced per milligram of rime
171 at -5°C. The ice splinters produced by the representation of the Hallett Mossop process are the smallest allowable size
172 of ice in the model (i.e. 10^{-18} kg, volume radius $\sim 0.11 \mu\text{m}$). The rate of splinter production by the Hallett Mossop
173 process is based on the best available estimate of the efficacy of the mechanism (Connolly et al., 2006; Hallett and
174 Mossop, 1974; Mossop, 1985). In-situ cloud observations have frequently observed ICNC that could be explained by
175 the Hallett Mossop process, but the mechanism underlying the Hallett Mossop process as well as the ice particle
176 production rate remain uncertain and not well quantified (Field et al., 2017). A maximum splinter production rate of
177 350 per milligram of rimed material has been measured in a number of laboratory studies (Hallett and Mossop, 1974;
178 Mossop, 1985) and has been applied as the best estimate here and in previous modelling studies (Connolly et al.,
179 2006), although other rates have also been measured (Heymsfield and Mossop, 1984; Saunders and Hosseini, 2001).
180 Uncertainties regarding the rate of splinter production by Hallett Mossop are an important consideration that will be
181 investigated in future work; this study explores the structural uncertainty of the presence/absence of the Hallett
182 Mossop process as currently understood. Other mechanisms of SIP such as collision fragmentation, droplet shattering
183 and sublimation fragmentation have been proposed (Field et al., 2017), but are not represented in these simulations,
184 in part because they are very poorly defined and it is not clear how important they are. Other studies have attempted
185 to model some of these additional SIP processes (Phillips et al., 2018; Sullivan et al., 2018) but that was beyond the
186 scope of this study.

187 **2.1.3. Cloud radiation**

188 The radiative processes are represented by the Suite of Community RAdiative Transfer codes based on Edwards and
189 Slingo (SOCRATES) (Edwards and Slingo, 1996; Manners et al., 2017), which considers cloud droplet number and mass,
190 as well as ice crystal and snow water paths for the calculation of cloud radiative properties. It does not respond to
191 changes in ice crystal or snow number concentration, or any changes to rain or graupel species. The cloud droplet
192 single scattering properties are calculated from the cloud droplet mass and effective radius in each gridbox using the
193 equations detailed in Edwards and Slingo (1996). Snow and ice are combined to form one ice category for the
194 purposes of the radiation calculations. The single scattering properties of this snow and ice category are calculated

195 from their combined mass and the ambient temperature. The parameterisation of bulk optical properties of snow and
196 ice used in the model is detailed in Baran et al. (2014).

197 The radiative properties (shortwave, longwave and total radiation) are calculated for daylight hours only, i.e. 10:00-
198 17:00 UTC. For all other modelled properties presented, except when plotted against a corresponding radiative
199 property, values are calculated for the last 14 hours of the simulation, i.e. from 10:00 - 24:00. The sensitivity of
200 analysis to time period selection was tested and found to have little impact.

201 Changes to outgoing radiation from cloudy regions and changes in cloud fraction both contribute to the total overall
202 change in outgoing radiation between two simulations. The contributions from changes in outgoing radiation from
203 cloudy regions and cloud fraction to the overall radiative differences between simulations were calculated separately
204 as described below. The cloudy regions contribution, i.e. the difference in outgoing radiation between two cloudy
205 regions due to changes in cloud albedo or thickness ignoring any changes in cloud fraction, (ΔRad_{REFL}) to a
206 domain radiative difference between ~~two simulations~~ a sensitivity simulation (s) and a reference simulation (r) ($s - r$)
207 is calculated using Eq. (1).

$$208 \quad \Delta Rad_{REFL} = cf_r \times \Delta Rad_{cl} \quad (1)$$

209 where cf_r is the cloud fraction of simulation r and ΔRad_{cl} is the change in outgoing radiation from cloudy areas only
210 between simulations ($s - r$). The reference run (r) in Sections 3.1 – 3.4 refers to the NoINP simulation while the sensitivity
211 run (s) are simulations which include an INP parameterisation. In Section 3.5, the reference run (r) refers to a simulation
212 which has no representation of SIP and the sensitivity run (s) to a simulation which includes SIP due to the Hallett
213 Mossop process. The cloud fraction contribution of cloud fraction changes, i.e. the change in radiation that can be
214 attributed to an area of clear sky in simulation s becoming cloudy in simulation r or vice versa, to the total change in
215 domain outgoing radiation (ΔRad_{CF}) is calculated using Eq. (2).

$$216 \quad \Delta Rad_{CF} = (Rad_{r,cl} - Rad_{r,cs}) \times \Delta cf \quad (2)$$

217 Where $Rad_{r,cl}$ is the mean outgoing radiation from cloudy regions in simulation r and $Rad_{r,cs}$ is the mean outgoing
218 radiation from clear sky regions in simulation r and Δcf is the difference in domain cloud fraction between simulations
219 s and r ($s - r$). There is interaction between the outgoing radiation from cloudy regions and cloud fraction changes
220 (ΔRad_{INT}) which is calculated in Eq (3).

221
$$\Delta Rad_{INT} = \Delta Rad_{cl} \times \Delta cf + \Delta Rad_{cs} \times (1 - cf_s) \quad (3)$$

222 Where ΔRad_{cs} is the change in mean outgoing radiation from clear sky areas between simulations s and r and cf_s is
 223 the cloud fraction of simulation s.

224 The total outgoing radiation difference between simulations s and r (ΔRad_{s-r}) is therefore as shown in Eq. (4).

225
$$\Delta Rad_{s-r} = Rad_s - Rad_r = \Delta Rad_{REFL} + \Delta Rad_{CF} + \Delta Rad_{INT} \quad (4)$$

226 The interaction term ΔRad_{INT} was found to be negligible and was therefore ignored for the purpose of this paper.

227 **2.1.4. Model simulations**

228 The conducted simulations are as follows:

- 229 - Five simulations with different heterogeneous ice nucleation parameterisations (C86, M92, D10, N12 and
 230 A13) with a representation of the Hallett Mossop process (SIP_active).
- 231 - One simulation with no heterogeneous ice nucleation (NoINP), but with a representation of the Hallett
 232 Mossop process (SIP_active).
- 233 - Five simulations with different heterogeneous ice nucleation parameterisations (C86, M92, D10, N12 and
 234 A13) without a representation of the Hallett Mossop process (SIP_inactive).

235 The INP number concentration ([INP]) predicted by the five INP parameterisations (C86, M92, D10, N12, A13) are
 236 compared with the available measurements from the study region (Price et al., 2018; Welti et al., 2018) in ~~Fig. 1~~Fig. 2,
 237 including those taken during the ICE-D field campaign (Price et al., 2018). All parameterisations are in reasonable
 238 agreement with the measurements (and with each other) at around -17°C, but deviate strongly at higher and lower
 239 temperatures. It should be noted that all parameterisations tested in this work were developed between specific
 240 temperature ranges and extrapolation beyond these temperatures adds uncertainty. However, for the purposes of
 241 this paper and to allow a direct comparison between parameterisations, all parameterisations have been applied
 242 between 0 and -37°C. Importantly, the INP parameterisation slopes of the chosen parameterisations span the range
 243 used within regional models (from a shallow $d\log_{10}[INP]/dT = -0.07$ in M92 (Meyers et al., 1992) to a steep
 244 $d\log_{10}[INP]/dT = -0.45$ in A13 (Atkinson et al., 2013)).

245 When analysing the simulation output, cloudy grid boxes were classed as those containing more than 10^{-5} kg kg⁻¹
246 condensed water from cloud droplets, ice crystals, graupel and snow. Rain was not included to ensure analysis did not
247 include areas below cloud base. Other cloud thresholds were tested and found to have no notable effect on the
248 results. For cloud categorisation into low, mid and high clouds, model vertical columns containing cloudy grid boxes
249 were categorised by cloud altitude. Low cloud occurs below 4km, mid cloud between 4 and 9 km and high cloud above
250 9 km. Columns with cloudy grid boxes in two or more cloud categories were classified as mixed category columns
251 according to the vertical placement of the cloudy grid boxes, e.g. low/high for columns containing cloud below 4 km
252 and above 9 km. 4 and 9 km were chosen as the low/mid and mid/high division points because they are just below
253 two well-defined peaks in cloud base heights (not shown) and roughly correspond to the beginning of the
254 heterogeneous and homogeneous freezing regions, respectively.

255 **2.2. The observed case**

256 MODIS visible images of the 21st August 2015 are shown in ~~Fig. 2~~Fig. 3 (a, b) alongside ~~a time series of snapshots of the~~
257 TOA outgoing longwave radiation in our one of our simulations (~~c, d-h~~). The simulated cloud field has more cloud-
258 free areas than the satellite images but in general produces clouds similar to those shown in the satellite image and in
259 approximately the correct location. Overall the simulations produce a complex and realistic cloud field. Snapshots of
260 the simulated model TOA outgoing shortwave radiation are shown in ~~Fig. A2~~Fig. A1.

261 In-situ measurements of cloud and aerosol properties were made using the UK FAAM Bae-146 research aircraft, which
262 was flown from Praia, Cape Verde Islands. An extensive suite of in-situ aerosol and cloud particle instruments were
263 operated onboard the aircraft and are described in detail in Lloyd et al. (2019). The aircraft penetrated the growing
264 convective clouds at a range of altitudes from just below the freezing level up to -20°C. In order to show that the
265 model reproduces the observed conditions, the observational data were compared to the conditions in modelled
266 clouds of similar size to those the aircraft flew in (10 – 150 km²) where a comparison was thought appropriate.

267 Comparisons of a selection of simulated cloud properties with aircraft data are shown in ~~Fig. A3~~Fig. A2. In-cloud
268 measurements from the aircraft were selected using the same total water content threshold as for the model data
269 (10^{-5} kg kg⁻¹). Note that observational data only samples clouds along the 1D flight path, while model results include all
270 grid points inside the selected clouds.

271 The vertical wind and cloud droplet and ice number concentrations are shown ~~Fig. A3~~Fig. A2. The vertical wind speeds
272 from the model and aircraft measurements agree well (~~Fig. A3~~Fig. A2a). The aircraft data exhibit less measurements of

273 vertical wind speeds above 10 m s^{-1} but that is expected since the aircraft was purposefully not flown in very high
274 updraft speeds. The aircraft cloud droplet number concentration (CDNC), measured using a DMT cloud droplet probe,
275 falls predominantly in the regions of parameter space most highly populated by model data when plotted against
276 vertical wind speed (Fig. A3Fig. A2b). Note that the simulated points in Figure A1b represent values of CDNC and
277 updraft speed in all cloudy gridboxes, not just those at cloud base. The updraft speed is collocated with CDNC and
278 therefore does not necessarily represent the updraft speed at which the cloud droplets were activated. The higher
279 CDNC values exhibited in the model data may be due to the higher updraft speeds which were not measured by the
280 aircraft. The observed ICNC was derived from measurements using the DMT Cloud Imaging Probes (CIP-15 and CIP-
281 100) and the SPEC Stereoscopic optical array probe covering a size range from 10 to $6200 \mu\text{m}$ using the SODA2
282 processing code to reconstruct ice particle images that are fully contained within the probe sample volume. Because
283 of uncertainties in the optical array probe sample volume for very small images, only ice particle images greater than
284 $100 \mu\text{m}$ were included. The aircraft ICNC fall almost entirely within the range of the model values (Fig. A3Fig. A2c).

285

286 3. Results

287 3.1. Effect of INP and INP parameterisation on outgoing radiation

288

289 We first examine the effect of INP parameterisation on the outgoing radiation relative to the simulation where the
290 only source of primary ice production was through homogeneous freezing (NoINP). Ice crystals formed via
291 homogeneous freezing can sediment to lower levels and initiate ice production via the Hallett Mossop process. When
292 contrasting the effect of different INP parameterisations in Sect 3.1-3.4, the Hallett Mossop process was always active
293 including in the NoINP simulation. As stated in Sect. 2.1.3, the radiation code is represented by the Suite Of
294 Community RAdiative Transfer codes based on Edwards and Slingo (SOCRATES) (Edwards and Slingo, 1996; Manners
295 et al., 2017), and responds to changes in cloud droplet number and cloud droplet, ice crystal and snow mass. The
296 results detailed below relate to either the domain-wide properties or all in-cloud regions within the domain. This
297 means that the results describe the direct and indirect changes, for example changes to the Hallett Mossop ice
298 production, occurring due to the presence of INP across all cloud present in the domain, including low-level liquid
299 clouds, mixed-phase clouds without a convective anvil and very deep convective clouds with an anvil. The effects of
300 INP parameterisation and SIP on convective anvils are discussed in Sect. 3.4.

301 Domain-mean TOA outgoing radiation (daylight hours, shortwave plus longwave) is enhanced by the inclusion of INP
302 in all cases (Fig. 3Fig. 4a). The enhancement in outgoing radiation varies between 2.6 W m⁻² for D10 and 20.8 W m⁻²
303 for A13 relative to the NoINP simulation. There is a variation of up to 18.2 W m⁻² depending on the chosen
304 representation of heterogeneous ice nucleation, which shows that the INP parameterisation can affect outgoing
305 radiation as much as excluding or including heterogeneous freezing altogether. ~~Radiative changes from the NoINP
306 simulation due to the inclusion of INP~~The difference in radiation between the NoINP and the simulations where INP
307 are present are caused mainly by changes to outgoing shortwave radiation. The inclusion of INP enhances outgoing
308 shortwave radiation by between 5.3 W m⁻² for D10 and 26.6 W m⁻² for A13 (Fig. A4Fig. A3a). Differences in outgoing
309 longwave radiation are comparatively small (-2.7 W m⁻² for D10 to -5.8 W m⁻² for A13; Fig. A4Fig. A3b) due to similar
310 cloud top heights between simulations of these thermodynamically limited clouds. Bear in mind that SIP was active
311 (SIP_active) in the simulations summarised in Fig. 3Fig. 4a, including in the NoINP simulation in which the Hallett
312 Mossop process can be initiated by settling ice crystals, indicating that these cloud systems are sensitive to INP even in
313 the presence of SIP. This is consistent with a comparatively small change in TOA radiation when SIP is active relative to
314 when it is inactive (Fig. 3Fig. 4b and 3c) (we discuss the role of SIP in more detail in Sect. 3.5).

315 The slope of the INP parameterisation (i.e. the dependence of INP number concentration on temperature) is a key
316 determinant of the outgoing radiation. There is a statistically significant correlation between INP parameterisation
317 slope and total TOA outgoing radiation ($r^2 = 0.75$, $p < 0.01$, $n = 10$) (Fig. 3Fig. 4c). Changes in outgoing radiation due to
318 the presence of INP are caused by a combination of changes to the outgoing radiation from cloudy regions, caused by
319 changes in cloud structure and microphysical properties, and changes to domain cloud fraction, whose contributions
320 to the total radiative difference are shown in Fig. 3Fig. 4a (left and centre). In order to appreciate the reasons for
321 these trends, we will now take a closer look at the effect of INP on outgoing radiation from cloudy regions only,
322 domain cloud fraction and cloud type.

323 **3.2. Effect of INP and INP parameterisation on outgoing radiation from cloudy regions**

324 Here we discuss the changes in outgoing radiation from cloudy regions only due to INP parameterisation choice.
325 Daytime outgoing radiation from cloudy regions increases due to INP for all but one INP parameterisation (Fig. 4Fig.
326 5a). The absolute change in outgoing radiation from cloudy regions is between -0.8 (D10) and +28.1 (A13) W m⁻², and
327 the larger values are a result of large increases in reflected shortwave (up to +37.2 W m⁻²) and relatively moderate
328 decreases in outgoing longwave radiation (up to -11.1 W m⁻²) from cloudy regions. The above absolute changes in

329 outgoing radiation from cloudy regions contribute between -0.7 and $+11.4 \text{ W m}^{-2}$ to the domain-mean change in
330 outgoing radiation due to the presence of INP (Fig. 3Fig. 4a, cloudy regions contribution).

331 The enhancement of outgoing radiation from cloudy regions due to INP is caused primarily by increases in cloud
332 condensate relative to the NoINP simulation (Fig. 4Fig. 5b). When INP are included in a simulation, snow and cloud
333 droplet water path are enhanced, causing increases in total cloud condensate, despite decreases (in all except A13) in
334 ice crystal water path due to a reduction in ice crystal number and mass concentrations due a reduction in the
335 availability of cloud droplets for homogeneous freezing. Snow, cloud droplets and ice crystals are the hydrometeors
336 that affect outgoing radiation in CASIM and the combined water path of these three species is significantly positively
337 correlated with cloud shortwave reflectivity ($r^2 = 0.62$, $p < 0.01$, $n = 11$) (Fig. 4Fig. 5c). The mechanism for this INP
338 induced increase in cloud condensate and consequently cloud shortwave reflectivity is as follows: When
339 heterogeneous ice nucleation is active, liquid is consumed in the warmer regions of mixed-phase clouds because of
340 increased heterogeneous ice nucleation (Fig. 1Fig. 2) and SIP (Fig. A5Fig. A4a). The resultant additional ice crystals in
341 mixed-phase regions facilitate riming causing increases in snow and graupel (Fig. A5Fig. A4c, d), increasing snow water
342 path and reflectivity in mixed-phase and ice clouds. At the same time, the enhanced production of relatively heavy
343 snow and graupel increases precipitation which on melting to form rain below the freezing level and subsequent
344 evaporation below 4 km, reduces out-of-cloud temperature and increases relative humidity (Fig. A6Fig. A5a, b). This
345 leads to increases in water path in low-level liquid clouds and thus an enhancement in their shortwave reflectivity.

346 However, increases in total cloud condensate alone cannot account for the differences in outgoing radiation from
347 cloudy regions between simulations using different INP parameterisations, which are caused by a combination of
348 cloud microphysical responses. We find that outgoing radiation from cloudy regions is significantly negatively
349 correlated with INP parameterisation slope ($r^2 = 0.63$, $p < 0.01$, $n = 10$) (Fig. 5Fig. 6a), i.e. simulations using a steep INP
350 parameterisation have a higher outgoing radiation from cloudy regions. This result makes sense when we consider the
351 relationships between INP parameterisation slope and a multitude of cloud microphysical properties affecting cloud
352 radiative properties. In particular, a steep INP parameterisation results in a mixed-phase cloud region characterised by
353 a higher ice crystal water path aloft ($r^2 = 0.80$, $p < 0.01$, $n = 10$; Fig. 5Fig. 6b) and higher cloud droplet number
354 concentrations at the bottom of the mixed-phase region ($r^2 = 0.89$, $p < 0.01$, $n = 10$; Fig. 5Fig. 6c) when compared to
355 shallower parameterisations. A steeper INP parameterisation slope allows increased transport of liquid to upper cloud
356 levels due to lower rates of heterogeneous freezing at the mid-bottom region of the mixed-phase cloud (lower
357 supercooling, (Fig. 1Fig. 2) and SIP at high temperatures (Fig. A5Fig. A4a). This, combined with higher INP

358 concentrations at low temperatures (Fig. 4), increases ICNC at upper mixed-phase altitudes, as well as enhancing
359 the lifetime of liquid cloud droplets at lower altitudes in the mixed-phase region when compared to shallower INP
360 parameterisations.

361 **3.3. Effect of INP and INP parameterisation on cloud fraction**

362 Overall cloud fraction is increased by INP for all INP parameterisations and these increases in cloud fraction contribute
363 about as much to changes in domain-mean radiation as the changes in outgoing radiation from cloudy regions (Fig.
364 3, cloud fraction contribution). Increases in domain cloud fraction due to INP are driven by cloud cover
365 increases in the warm and mixed-phase regions of the cloud (~ 4 -6 km), offset somewhat by decreases in the cloud
366 fraction due to reduced homogeneous freezing in the ~ 10 - 14 km regime (~~~ 10 - 14 km~~) (Fig. 6, 7a). Cloud fraction
367 increases at mid-levels occur because heterogeneous ice nucleation induces an increase in precipitation-sized
368 particles (snow and graupel) which sediment to lower levels and moisten the atmosphere by evaporation (Fig. A6, Fig.
369 A5a, b). This increases new cloud formation and may prolong the lifetime of existing cloud cells. Additionally,
370 increased droplet freezing and riming in the mixed-phase cloud region releases latent heat and invigorates cloud
371 development with increases in updraft speed just above 4 km (Fig. A6, Fig. A5c). The increased cloud fraction at mid-
372 levels due to INP are partially offset by a reduced cloud fraction above 10 km (Fig. 6, Fig. 7a) which is caused by an INP
373 induced enhancement in freezing and riming in the mixed-phase region reducing moisture transport to the
374 homogeneous freezing regime.

375 The effects of INP on the altitude profile of cloud fraction are strongest for shallow INP parameterisation slopes, which
376 have a freezing profile most different to that of the NoINP simulation (Fig. 6, Fig. 7a). At 5 km, the shallowest
377 parameterisation (M92) causes the largest increase in cloud fraction, while the steepest parameterisation (A13)
378 causes the smallest ($r^2 = 0.83$, $p < 0.05$, $n = 5$). At 12 km, the order is reversed, and steep parameterisations exhibit the
379 highest cloud fraction ($r^2 = 0.94$, $p < 0.01$, $n = 5$). The largest cloud fraction-induced increases in outgoing radiation
380 relative to the NoINP simulation (Fig. 3, Fig. 4a) are seen in simulations using steeper INP parameterisations because
381 these simulations exhibit higher cloud fractions at high altitudes (~12 km), translating into the higher total cloud
382 fraction. These slope dependent changes in cloud fraction are explained by a relationship between cloud fraction and
383 several microphysical properties affecting cloud fraction. For example, steeper INP parameterisations produce higher
384 ICNC at the top of the mixed-phase region (10 km) as well as higher ratios of ice crystal mass to snow and graupel
385 mass within the homogeneous freezing region (12 km) (Fig. 6, Fig. 7b, c). A higher number and mass of ice crystals

386 relative to those of larger precipitation-sized hydrometeors with the steepest parameterisations results in lower
387 frozen hydrometeor sedimentation, a longer cloud lifetime and a higher cloud fraction.

388 **3.4. Effect of INP and INP parameterisation on cirrus anvils**

389 Our results show that the INP parameterisation affects the properties and spatial extent of cirrus anvils. We define
390 cirrus anvils to be regions where cloud is present above 9 km only (further details available in Sect. 2.1.4). 2D aerial
391 images of cloud categorisation (Fig. 7 Fig. 8a-f) show well-defined regions of anvil cloud (light blue - H) surrounding a
392 large convective system containing clouds at a range of altitudes from <4 km to >9 km. There are clearly differences in
393 the extent and position of cloud categories between simulations (Fig. 7 Fig. 8a -f).

394 The presence of INP reduces convective anvil extent by between 2.1 and 4.1% of the domain area depending on the
395 choice of INP parameterisation (Fig. 7 Fig. 8 g), corresponding to a decrease in anvil cloud of between 22 and 53%
396 relative to the NoINP simulation (not shown). The reduction in anvil extent in the presence of INP is caused by
397 increased liquid consumption at all mixed-phase levels, due to heterogeneous freezing, enhanced SIP and increased
398 graupel and snow production, reducing the availability of cloud droplets for homogeneous freezing (Fig. A5 Fig. A4b),
399 reducing ICNC at cloud-top, and reducing cloud anvil extent (Fig. 7 Fig. 8g).

400 Reductions in anvil extent caused by INP are somewhat offset by the overall increases in cloud fraction across the
401 domain (Fig. 7 Fig. 8g). However, it is possible that the effect of INP and INP parameterisation choice on anvil cloud
402 fraction, and the contribution of anvil cloud to overall cloud fraction and radiative changes, would become larger with
403 a longer analysis period. This is because detrained convective anvils can persist longer in the atmosphere than the
404 convective core that creates them (Luo and Rossow, 2004; Mace et al., 2006), but this is beyond the scope of the
405 current study.

406 **3.5. Importance of secondary ice production**

407 It has been argued that the observed (or derived) primary ice particle production rate is unimportant for convective
408 cloud properties when secondary ice production (SIP) is active (Fridlind et al., 2007; Heymsfield and Willis, 2014;
409 Ladino et al., 2017; Lawson et al., 2015) because primary ice crystal concentrations are often overwhelmed by ice
410 crystals formed via SIP (Field et al., 2017). However, the results shown in Fig. 3 Fig. 4a (in which the simulations
411 included SIP) do not support this argument. We find that the microphysical and radiative properties of the cloud field
412 depend strongly on the properties of the INP even ~~with~~ when SIP due to the ~~{Hallett-Mossop process}~~ occurs.
413 Furthermore, the effect of including SIP on daylight domain-mean outgoing radiation varies between -2.0 W m^{-2} and

414 +6.6 W m⁻² (Fig. 3Fig. 4b), showing that SIP the presence of the Hallett Mossop process has a smaller effect than the
415 INP parameterisation. Furthermore, the and that the sign and magnitude of this effect of SIP depends on the INP
416 parameterisation. The mean effect on daylight domain-mean outgoing radiation of including INP is +9.8 W m⁻²
417 whereas the mean effect of including SIP via the Hallett Mossop process is +2.9 W m⁻². Therefore, rather than primary
418 ice being simply overwhelmed by SIP, it actually determines how SIP affects cloud microphysics. Other mechanisms of
419 SIP have been proposed (Field et al., 2017; Lauber et al., 2018) and the impact of INP on cloud properties in the
420 presence of these mechanisms, particularly those present at temperatures below 10°C such as droplet shattering
421 (Lauber et al., 2018), should be tested in future but this was beyond the scope of the present study.

422 The effect of SIP on the radiative properties of the cloud field is dependent on INP parameterisation choice, both in
423 magnitude and sign of change (Fig. 3Fig. 4b). SIP makes the clouds more reflective independent of the chosen
424 parameterisation (Fig. 3Fig. 4b, cloudy regions contribution) due to increases in snow and cloud droplet water path.
425 N12 and A13 have the largest overall radiative response to SIP because changes to the radiative forcing from cloudy
426 regions and cloud fraction contributions act to increase outgoing radiation (Fig. 3Fig. 4b). However, the cloud fraction
427 response to SIP is opposite for C86, M92 and D10 meaning the cloudy regions and cloud fraction contributions act in
428 opposite directions, reducing the total radiative forcing.

429 The different response of the domain cloud fraction to the presence of SIP is caused by substantial variation between
430 simulations in the anvil cloud extent (Fig. 7Fig. 8h), from an increase of 10% (+0.9% of the domain area) in N12 to a
431 decrease of 40% (-3.6% of the domain area) in M92 (Fig. 7Fig. 8h). These non-uniform changes in cloud fraction and
432 outgoing radiation can be explained by differences in the response of cloud freezing profiles to SIP due to variations in
433 INP parameterisation slope. For all INP parameterisations, SIP reduces the availability of liquid at higher altitudes. For
434 shallower parameterisations such as M92 this causes a reduction in the amount of cloud droplets reaching the
435 homogeneous freezing regime and thereby reduces ICNC and cloud anvil spatial extent. However, in simulations using
436 a steep parameterisation, almost all available droplets are frozen heterogeneously before they reach the
437 homogeneous regime (see reduced homogeneous ice production rates in N12 and A13 in Fig. A5Fig. A4b). Therefore,
438 in simulations using a steeper parameterisation, such as N12, a reduction in liquid availability due to SIP occurs at the
439 top of the heterogeneous freezing regime, reducing the availability of liquid for riming, causing a reduction in frozen
440 hydrometeor size at high altitudes, a reduction in hydrometeor sedimentation and an increase in anvil extent. The
441 effects of INP parameterisation slope and the Hallett Mossop process on the simulated cloud field properties are
442 summarised in Fig. 9. Overall, our simulations show that INP parameterisation choice and slope is an important

443 determinant of cloud field micro- and macrophysical properties, even when SIP is active, and that choice of INP
444 parameterisation affects the cloud field response to SIP.

445

446 **4. Limitations of this modelling study**

447 The lack of consideration of ice and snow particle number by the SOCRATES radiation scheme is an important
448 limitation of the results presented here. Changes to ICNC, without a co-occurring change in ice crystal mass
449 concentrations, will not be reflected in modelled radiative fluxes. However, our results are still very relevant for
450 climate model simulations as climate models do not typically ~~represent~~ account for ICNC in their radiation
451 calculations and have frequently been shown to poorly represent ice crystal mass concentrations (Baran et al., 2014;
452 Waliser et al., 2009). The SOCRATES representation of radiation with a dependence on ice mass is a more accurate
453 and realistic representation of radiation than is seen in many climate models which often derive bulk optical
454 properties using empirically derived deterministic relationships between ice particle size and environmental
455 temperature and/or ice water content (Baran et al., 2014; Edwards et al., 2007; Fu et al., 1999; Gu et al., 2011).
456 However, the effect of INP parameterisation on deep convective clouds radiative properties using a radiation code
457 that considers ice particle number should be explored in future studies. The sensitivity of the cloud field to the chosen
458 INP parameterisation and SIP indicates the importance of accurately representing ice water content in climate models
459 and linking this ice water content to ice-nucleating particle type.

460 Another limitation of the SOCRATES radiation code is its lack of consideration of rain and graupel particles. The effects
461 of these hydrometeors are expected to be less than that of ice, snow and cloud droplets as they precipitate faster and
462 therefore have a shorter lifetime. Furthermore, the effect of graupel on the tropical longwave radiative effect has
463 been found to be negligible and dwarfed by that of snow (Chen et al., 2018). The global radiative effect of rain has also
464 been found to be small in the vast majority of cases even at high temporal and spatial resolution (Hill et al., 2018). The
465 effect of the incorporation of these hydrometeors into radiative transfer parameterisations should however be tested
466 in future studies.

467 The use of both aerosol-dependent (D10, N12, A13) and solely-temperature dependent (C86, M92) parameterisations
468 in this study means that we have examined the radiative sensitivity of a complex cloud field to a larger variety of INP
469 parameterisations used in weather and climate models than if we had exclusively used parameterisations that

470 consider aerosol concentration. However, this experimental design has limitations. For example, due to the lack of
471 aerosol dependence of the C86 and M92 schemes a 'presumed' dust concentration is implicitly present in these two
472 cases and remains uniform throughout the simulation period. The effect of INP parameterisation choice on convective
473 cloud field properties should also be examined with the inclusion of aerosol scavenging but this was beyond the scope
474 of this study.

475 This study utilised our best estimate of ice production by the Hallett Mossop process (Connolly et al., 2006; Hallett and
476 Mossop, 1974; Mossop, 1985), the most well-studied SIP mechanism, to try and understand the effect of the process,
477 as currently understood, on deep convective cloud properties. The work indicates that INP concentrations at all mixed
478 phase temperatures can be important for cloud properties even in the presence of the Hallett Mossop process, and
479 that the impact of the Hallett Mossop process depends on INP number concentrations. The dependence of the rate of
480 ice production by the Hallett Mossop process on INP number concentrations (Figure A5a) in particular highlights that
481 the role of SIP in clouds may be dependent on INP. However, ~~this~~ the rate of ice production by the Hallett Mossop
482 process is very uncertain and other mechanisms of SIP have also been proposed (Field et al., 2017). We recommend
483 that similar studies examining the effect of INP should be conducted with the inclusion of other proposed SIP
484 mechanisms, particularly those that may be present at temperatures below -10°C, such as droplet shattering (Lauber
485 et al., 2018). However, this was beyond the scope of the present study due in part to the lack of quantification and
486 parameterisations for these other mechanisms (Field et al., 2017). -Future work will attempt to overcome the above
487 caveats by using statistical emulation (Johnson et al., 2015b) to examine the interacting effects of dust number
488 concentration, INP parameterisation slope and SIP in an idealised deep convective cloud.

489

490 **5. Conclusions**

491 We quantified the effect of INP parameterisation choice on the radiative properties of a deep convective cloud field
492 using a regional model with advanced double-moment capabilities. The simulated domain exceeds 600,000 km² and
493 therefore captures the effects of INP and INP parameterisation on a typical large, complex and heterogeneous
494 convective cloud field. The presence of INP increases domain-mean daylight TOA outgoing radiation by between 2.6
495 and 20.8 W m⁻² and the choice of INP parameterisation can have as large an effect on cloud field properties as the
496 inclusion or exclusion of INP. These effects are evident even in the presence of SIP due to the Hallett Mossop process,

497 refuting the hypothesis that INP is irrelevant beyond a minimum concentration needed to initiate ~~SIP~~the Hallett
498 Mossop process (Crawford et al., 2012; Ladino et al., 2017; Phillips et al., 2007). An important caveat of this result is
499 that other SIP mechanisms, such as droplet shattering (Ladino et al., 2017; Lauber et al., 2018), are not represented in
500 our model simulations. Furthermore, the effects of SIP on the cloud field properties are strongly dependent on INP
501 parameterisation choice. Both the magnitude and direction of change in cloud fraction and total outgoing radiation
502 due to SIP varies according to INP parameterisation choice. Microphysical alterations to cloud properties are
503 important contributors to radiative differences between simulations, in agreement with previous studies documenting
504 the effect of aerosol-cloud interactions to the radiative forcing by deep convective clouds (Fan et al., 2013). For
505 example, increasing cloud condensation nuclei concentrations, with no perturbations to INP, was shown to increase
506 cloud albedo and cloud fraction, deepen clouds and increase TOA outgoing radiation by 2-4 W m⁻² (Fan et al., 2013).
507 Here we find that even for the same aerosol and CCN concentrations, just altering the relationship between aerosol
508 concentration and ice-nucleating ability can cause changes in daylight TOA outgoing radiation of up to 18.2 W m⁻² in
509 our domain.

510 Our results indicate that the slope of the INP parameterisation with respect to temperature ($d\log[\text{INP}]/dT$) is
511 particularly important: Outgoing total radiation, along with many cloud field and microphysical properties affecting
512 radiation, were significantly correlated with INP parameterisation slope. Best practise for accurately representing INP
513 number concentrations based on current knowledge is to utilise parameterisations that link aerosol number and
514 particle size to INP number concentration (e.g. D10, N12, A13) but that is not enough without also using a
515 parameterisation in which the temperature dependence of the INP number concentrations matches reality; the
516 largest differences in domain outgoing radiation existed in this study between simulations using aerosol dependent
517 parameterisations (D10 and A13). These large variations in outgoing radiation between simulations using different
518 aerosol dependent INP parameterisations justifies investment in observational campaigns to more effectively
519 constrain the range of expected INP concentrations and parameterisation slopes in the Saharan dust outflow region,
520 and other regions dominated by maritime deep convective activity.

521 The significance of the slope of the INP parameterisation indicates the potential importance of accounting for
522 differences in aerosol composition in modelling studies. For example, INP derived from marine organics (Wilson et al.,
523 2015) have a shallower slope than mineral dust INP (Atkinson et al., 2013; Niemand et al., 2012). Furthermore, real-
524 world INP concentrations are known to have complex temperature dependencies with biological INP, such as soil
525 borne fungus and plant related bacteria, making significant contributions at the warmest temperatures and mineral

526 components being more important at lower temperatures (O'Sullivan et al., 2018). The work here suggests that the
527 presence of biological INP might be to reduce liquid water transport to the upper levels of the cloud, reducing cirrus
528 anvil extent, but also to increase low cloud fraction. Nevertheless, measurements in the eastern tropical Atlantic
529 indicate that biological INP in the Saharan dust plumes is at most a minor contribution and that the parameterisations
530 with shallow slope in ~~Fig. 1~~Fig. 2 produce too much glaciation at warm temperatures.

531 The results presented here also present a new framework for understanding the effect of SIP by identifying a potential
532 relationship between the effect of the Hallett Mossop process and INP parameterisation slope. The significance of INP
533 parameterisation slope also highlights the importance of characterising the INP concentration across the entirety of
534 the mixed-phase temperature range rather than just at one temperature, or in a narrow temperature range, as is
535 common in many field campaigns. For example, in the ICE-D field campaign, INP concentrations at temperatures
536 above -7 and below -27°C were not measurable due to experimental and sampling constraints (Price et al., 2018).
537 Measuring INP over the entire mixed-phase temperature range, throughout which deep convective clouds extend,
538 conceivably covering around 10 orders of magnitude in INP number concentration, represents a major experimental
539 challenge. This issue is compounded by the fact that INP spectra cannot reliably be extrapolated to higher or lower
540 temperatures since our underpinning physical understanding of what makes an effective nucleation site is lacking
541 (Coluzza et al., 2017; Holden et al., 2019; Kanji et al., 2017). This work demonstrates the importance of solving these
542 problems and measuring INP number concentrations across the entirety of the mixed-phase temperature spectrum,
543 as has been demonstrated in previous work (e.g. Liu et al., 2018; Takeishi and Storelvmo, 2018).

544 **Data Availability**

545 The datasets generated and analysed in this study are available from the corresponding author on reasonable request.

546 **Author Contributions**

547 REH, AKM, KSC, PRF and BJM contributed to the design, development and direction of the study. REH and AKM set up
548 and ran the UM-CASIM simulations presented in the paper. REH processed and analysed the UM-CASIM datasets.
549 JMW, AAH and BJS built and maintained the Met-Office CASIM model used to run the simulations. ZC and RJC
550 provided processed aircraft data from the ICE-D b933 flight and helped with the comparison of model data with
551 aircraft measurements. REH, AKM, JMW, AAH, ZC, RJC, KSC, PRF and BJM edited the manuscript.

552 **Competing interests**

553 The authors declare no competing interests.

554 **Acknowledgements**

555 This work has been funded by European Research Council (ERC, grant 648661 MarineIce) and the Natural Environment
556 Research Council (NERC, grant NE/M00340X/1). We acknowledge the use of Monsoon, a collaborative High
557 Performance Computing facility funded by the Met Office and NERC. We acknowledge the use of JASMIN, the UK
558 collaborative data analysis facility. We obtained moderate resolution imaging spectroradiometer (MODIS) Corrected
559 Reflectance images from the NASA Worldview website (<https://worldview.earthdata.nasa.gov/>). Airborne
560 measurements were obtained from the ICE-D field campaign and specifically the b933 flight on the 21st August 2015.
561 The ICE-D campaign used the BAe-146-301 Atmospheric Research Aircraft which is operated by Directflight Ltd (now
562 Airtask) and managed by the Facility for Airborne Atmospheric Measurements (FAAM). At the time of the
563 measurements FAAM was a joint entity of NERC and the UK Met Office. We thank all the people involved in the ICE-D
564 campaign.

565 **References**

- 566 Abdul-Razzak, H. and Ghan, S. J.: A parameterization of aerosol activation: 2. Multiple aerosol types, *J. Geophys. Res.*,
567 105(16), 6837–6844, doi:10.1029/1999JD901161, 2000.
- 568 Arakawa, A.: The cumulus parameterization problem: Past, present, and future, *J. Clim.*, 17(13), 2493–2525,
569 doi:10.1175/1520-0442(2004)017<2493:RATCPP>2.0.CO;2, 2004.
- 570 Atkinson, J. D., Murray, B. J., Woodhouse, M. T., Whale, T. F., Baustian, K. J., Carslaw, K. S., Dobbie, S., O’Sullivan, D.
571 and Malkin, T. L.: The importance of feldspar for ice nucleation by mineral dust in mixed-phase clouds, *Nature*,
572 498(7454), 355–358, doi:10.1038/nature12278, 2013.
- 573 Baran, A. J., Hill, P., Furtado, K., Field, P. and Manners, J.: A Coupled Cloud Physics–Radiation Parameterization of the
574 Bulk Optical Properties of Cirrus and Its Impact on the Met Office Unified Model Global Atmosphere 5.0 Configuration,
575 *J. Clim.*, 27(20), 7725–7752, doi:10.1175/JCLI-D-13-00700.1, 2014.
- 576 Bigg, E. K.: The formation of atmospheric ice crystals by the freezing of droplets, *Q. J. R. Meteorol. Soc.*, 79(342), 510–
577 519, doi:10.1002/qj.49707934207, 1953.
- 578 Boose, Y., Kanji, Z. A., Kohn, M., Sierau, B., Zipori, A., Crawford, I., Lloyd, G., Bukowiecki, N., Herrmann, E., Kupiszewski,
579 P., Steinbacher, M. and Lohmann, U.: Ice nucleating particle measurements at 241K during winter months at 3580m
580 MSL in the swiss alps, *J. Atmos. Sci.*, 73(5), 2203–2228, doi:10.1175/JAS-D-15-0236.1, 2016a.
- 581 Boose, Y., Sierau, B., García, M. I., Rodríguez, S., Alastuey, A., Linke, C., Schnaiter, M., Kupiszewski, P., Kanji, Z. A. and
582 Lohmann, U.: Ice nucleating particles in the Saharan Air Layer, *Atmos. Chem. Phys.*, 16(14), 9067–9087,
583 doi:10.5194/acp-16-9067-2016, 2016b.
- 584 Cantrell, W. and Heymsfield, A.: Production of ice in tropospheric clouds: a review, *Bull. Am. Meteorol. Soc.*, 86(6),
585 795–808, doi:10.1175/BAMS-86-6-795, 2005.
- 586 Carrió, G. G., van den Heever, S. C. and Cotton, W. R.: Impacts of nucleating aerosol on anvil-cirrus clouds: A modeling
587 study, *Atmos. Res.*, 84(2), 111–131, doi:10.1016/j.atmosres.2006.06.002, 2007.
- 588 Chen, Y., Seiki, T., Kodama, C., Satoh, M. and Noda, A. T.: Impact of Precipitating Ice Hydrometeors on Longwave
589 Radiative Effect Estimated by a Global Cloud-System Resolving Model, *J. Adv. Model. Earth Syst.*, 10(2), 284–296,
590 doi:10.1002/2017MS001180, 2018.
- 591 Coluzza, I., Creamean, J., Rossi, M., Wex, H., Alpert, P., Bianco, V., Boose, Y., Dellago, C., Felgitsch, L., Fröhlich-
592 Nowoisky, J., Herrmann, H., Jungblut, S., Kanji, Z., Menzl, G., Moffett, B., Moritz, C., Mutzel, A., Pöschl, U., Schauerl,
593 M., Scheel, J., Stopelli, E., Stratmann, F., Grothe, H. and Schmale, D.: Perspectives on the Future of Ice Nucleation
594 Research: Research Needs and Unanswered Questions Identified from Two International Workshops, *Atmosphere*
595 (Basel), 8(12), 138, doi:10.3390/atmos8080138, 2017.
- 596 Connolly, P. J., Choulaton, T. W., Gallagher, M. W., Bower, K. N., Flynn, M. J. and Whiteway, J. A.: Cloud-resolving
597 simulations of intense tropical Hector thunderstorms: Implications for aerosol-cloud interactions, *Meteorol. Soc.*, 132,
598 3079–3106, doi:10.1256/qj.05.86, 2006.
- 599 Cooper, W. A.: Ice initiation in natural clouds, in *Precipitation enhancement—A scientific challenge*, pp. 29–32,

600 American Meteorological Society, Boston, MA., 1986.

601 Crawford, I., Bower, K. N., Choulaton, T. W., Dearden, C., Crosier, J., Westbrook, C., Capes, G., Coe, H., Connolly, P. J.,
602 Dorsey, J. R., Gallagher, M. W., Williams, P., Trembath, J., Cui, Z. and Blyth, A.: Ice formation and development in aged,
603 wintertime cumulus over the UK: observations and modelling, *Atmos. Chem. Phys.*, 12(11), 4963–4985,
604 doi:10.5194/acp-12-4963-2012, 2012.

605 DeMott, P. J., Sassen, K., Poellot, M. R., Baumgardner, D., Rogers, D. C., Brooks, S. D., Prenni, A. J. and Kreidenweis, S.
606 M.: African dust aerosols as atmospheric ice nuclei, *Geophys. Res. Lett.*, 30(14), 1732–1726,
607 doi:10.1029/2003GL017410, 2003.

608 DeMott, P. J., Prenni, A. J., Liu, X., Kreidenweis, S. M., Petters, M. D., Twohy, C. H., Richardson, M. S., Eidhammer, T.
609 and Rogers, D. C.: Predicting global atmospheric ice nuclei distributions and their impacts on climate., *Proc. Natl. Acad.*
610 *Sci. U. S. A.*, 107(25), 11217–22, doi:10.1073/pnas.0910818107, 2010.

611 DeMott, P. J., Prenni, A. J., McMeeking, G. R., Sullivan, R. C., Petters, M. D., Tobo, Y., Niemand, M., Möhler, O., Snider,
612 J. R., Wang, Z. and Kreidenweis, S. M.: Integrating laboratory and field data to quantify the immersion freezing ice
613 nucleation activity of mineral dust particles, *Atmos. Chem. Phys.*, 15, 393–409, doi:10.5194/acp-15-393-2015, 2015.

614 Deng, X., Xue, H. and Meng, Z.: The effect of ice nuclei on a deep convective cloud in South China, *Atmos. Res.*, 206, 1–
615 12, doi:10.1016/J.ATMOSRES.2018.02.013, 2018.

616 Edwards, J. M. and Slingo, A.: Studies with a flexible new radiation code. I: Choosing a configuration for a large-scale
617 model, *Q. J. R. Meteorol. Soc.*, 122(531), 689–719, doi:10.1002/qj.49712253107, 1996.

618 Edwards, J. M., Havemann, S., Thelen, J. C. and Baran, A. J.: A new parametrization for the radiative properties of ice
619 crystals: Comparison with existing schemes and impact in a GCM, *Atmos. Res.*, 83(1), 19–35,
620 doi:10.1016/j.atmosres.2006.03.002, 2007.

621 Eidhammer, T., Demott, P. J. and Kreidenweis, S. M.: A comparison of heterogeneous ice nucleation parameterizations
622 using a parcel model framework, *J. Geophys. Res. Atmos.*, 114(6), doi:10.1029/2008JD011095, 2009.

623 Ekman, A. M. L., Engström, A. and Wang, C.: The effect of aerosol composition and concentration on the development
624 and anvil properties of a continental deep convective cloud, *Q. J. R. Meteorol. Soc.*, 133(627), 1439–1452,
625 doi:10.1002/qj.108, 2007.

626 Fan, J., Comstock, J. M. and Ovchinnikov, M.: The cloud condensation nuclei and ice nuclei effects on tropical anvil
627 characteristics and water vapor of the tropical tropopause layer, *Environ. Res. Lett.*, 5(4), 044005, doi:10.1088/1748-
628 9326/5/4/044005, 2010a.

629 Fan, J., Comstock, J. M., Ovchinnikov, M., McFarlane, S. A., McFarquhar, G. and Allen, G.: Tropical anvil characteristics
630 and water vapor of the tropical tropopause layer: Impact of heterogeneous and homogeneous freezing
631 parameterizations, *J. Geophys. Res.*, 115(D12), D12201, doi:10.1029/2009JD012696, 2010b.

632 Fan, J., Rosenfeld, D., Ding, Y., Leung, L. R. and Li, Z.: Potential aerosol indirect effects on atmospheric circulation and
633 radiative forcing through deep convection, *Geophys. Res. Lett.*, 39(9), L09806, doi:10.1029/2012GL051851, 2012.

634 Fan, J., Leung, L. R., Rosenfeld, D., Chen, Q., Li, Z., Zhang, J. and Yan, H.: Microphysical effects determine

635 macrophysical response for aerosol impacts on deep convective clouds., *Proc. Natl. Acad. Sci. U. S. A.*, 110(48), E4581-
636 90, doi:10.1073/pnas.1316830110, 2013.

637 Field, P. R., Lawson, R. P., Brown, P. R. A., Lloyd, G., Westbrook, C., Moisseev, D., Miltenberger, A., Nenes, A., Blyth, A.,
638 Choulaton, T., Connolly, P., Buehl, J., Crosier, J., Cui, Z., Dearden, C., DeMott, P., Flossmann, A., Heymsfield, A., Huang,
639 Y., Kalesse, H., Kanji, Z. A., Korolev, A., Kirchgaessner, A., Lasher-Trapp, S., Leisner, T., McFarquhar, G., Phillips, V.,
640 Stith, J., Sullivan, S., Field, P. R., Lawson, R. P., Brown, P. R. A., Lloyd, G., Westbrook, C., Moisseev, D., Miltenberger, A.,
641 Nenes, A., Blyth, A., Choulaton, T., Connolly, P., Buehl, J., Crosier, J., Cui, Z., Dearden, C., DeMott, P., Flossmann, A.,
642 Heymsfield, A., Huang, Y., Kalesse, H., Kanji, Z. A., Korolev, A., Kirchgaessner, A., Lasher-Trapp, S., Leisner, T.,
643 McFarquhar, G., Phillips, V., Stith, J. and Sullivan, S.: Chapter 7. Secondary ice production - current state of the science
644 and recommendations for the future, *Meteorol. Monogr.*, 7.1-7.20 [online] Available from:
645 <http://journals.ametsoc.org/doi/10.1175/AMSMONOGRAPHS-D-16-0014.1> (Accessed 4 April 2017), 2017.

646 Fridlind, A. M., Ackerman, A. S., McFarquhar, G., Zhang, G., Poellot, M. R., DeMott, P. J., Prenni, A. J. and Heymsfield,
647 A. J.: Ice properties of single-layer stratocumulus during the Mixed-Phase Arctic Cloud Experiment: 2. Model results, *J.*
648 *Geophys. Res.*, 112(D24), D24202, doi:10.1029/2007JD008646, 2007.

649 Fu, Q., Sun, W. B., Yang, P., Fu, Q., Sun, W. B. and Yang, P.: Modeling of Scattering and Absorption by Nonspherical
650 Cirrus Ice Particles at Thermal Infrared Wavelengths, [http://dx.doi.org/10.1175/1520-](http://dx.doi.org/10.1175/1520-0469(1999)056<2937:MOSAAB>2.0.CO;2)
651 [0469\(1999\)056<2937:MOSAAB>2.0.CO;2](http://dx.doi.org/10.1175/1520-0469(1999)056<2937:MOSAAB>2.0.CO;2), doi:10.1175/1520-0469(1999)056<2937:MOSAAB>2.0.CO;2, 1999.

652 Gibbons, M., Min, Q. and Fan, J.: Investigating the impacts of Saharan dust on tropical deep convection using spectral
653 bin microphysics, *Atmos. Chem. Phys*, 18, 12161–12184, doi:10.5194/acp-18-12161-2018, 2018.

654 Grosvenor, D. P., Field, P. R., Hill, A. A. and Shipway, B. J.: The relative importance of macrophysical and cloud albedo
655 changes for aerosol-induced radiative effects in closed-cell stratocumulus: insight from the modelling of a case study,
656 *Atmos. Chem. Phys*, 17, 5155–5183, doi:10.5194/acp-17-5155-2017, 2017.

657 Gu, Y., Liou, K. N., Ou, S. C. and Fovell, R.: Cirrus cloud simulations using WRF with improved radiation
658 parameterization and increased vertical resolution, *J. Geophys. Res.*, 116(D6), D06119, doi:10.1029/2010JD014574,
659 2011.

660 Hallett, J. and Mossop, S. C.: Production of secondary ice particles during the riming process, *Nature*, 249(5452), 26–
661 28, doi:10.1038/249026a0, 1974.

662 Harrison, A. D., Whale, T. F., Carpenter, M. A., Holden, M. A., Neve, L., O’Sullivan, D., Vergara Temprado, J. and
663 Murray, B. J.: Not all feldspars are equal: a survey of ice nucleating properties across the feldspar group of minerals,
664 *Atmos. Chem. Phys.*, 16(17), 10927–10940, doi:10.5194/acp-16-10927-2016, 2016.

665 Harrison, A. D., Lever, K., Sanchez-Marroquin, A., Holden, M. A., Whale, T. F., Tarn, M. D., McQuaid, J. B. and Murray,
666 B. J.: The ice-nucleating ability of quartz immersed in water and its atmospheric importance compared to K-feldspar,
667 *Atmos. Chem. Phys.*, 19(17), 11343–11361, doi:10.5194/acp-19-11343-2019, 2019.

668 van den Heever, S. C., Carrió, G. G., Cotton, W. R., DeMott, P. J. and Prenni, A. J.: Impacts of nucleating aerosol on
669 Florida storms. Part I: Mesoscale simulations, *J. Atmos. Sci.*, 63(7), 1752–1775, doi:10.1175/JAS3713.1, 2006.

670 Herbert, R. J., Murray, B. J., Dobbie, S. J. and Koop, T.: Sensitivity of liquid clouds to homogenous freezing

671 parameterizations, *Geophys. Res. Lett.*, 42(5), 1599–1605, doi:10.1002/2014GL062729@10.1002/(ISSN)1944-
672 8007.2015EDHIGHLIGHTS, 2015.

673 Heymsfield, A. and Willis, P.: Cloud conditions favoring secondary ice particle production in tropical maritime
674 convection, *J. Atmos. Sci.*, 71(12), 4500–4526, doi:10.1175/JAS-D-14-0093.1, 2014.

675 Heymsfield, A. J. and Mossop, S. C.: Temperature dependence of secondary ice crystal production during soft hail
676 growth by riming, *Q. J. R. Meteorol. Soc.*, 110(465), 765–770, doi:10.1002/qj.49711046512, 1984.

677 Hill, P. G., Chiu, J. C., Allan, R. P. and Chern, J. -D.: Characterizing the Radiative Effect of Rain Using a Global Ensemble
678 of Cloud Resolving Simulations, *J. Adv. Model. Earth Syst.*, 10(10), 2453–2470, doi:10.1029/2018MS001415, 2018.

679 Holden, M. A., Whale, T. F., Tarn, M. D., O’Sullivan, D., Walshaw, R. D., Murray, B. J., Meldrum, F. C. and Christenson,
680 H. K.: High-speed imaging of ice nucleation in water proves the existence of active sites, *Sci. Adv.*, 5(2),
681 doi:10.1126/sciadv.aav4316, 2019.

682 Huang, Y., Blyth, A. M., Brown, P. R. A., Choulaton, T. W. and Cui, Z.: Factors controlling secondary ice production in
683 cumulus clouds, *Q. J. R. Meteorol. Soc.*, 143(703), 1021–1031, doi:10.1002/qj.2987, 2017.

684 Jeffery, C. A. and Austin, P. H.: Homogeneous nucleation of supercooled water: Results from a new equation of state,
685 *J. Geophys. Res. Atmos.*, 102(21), 25269–25279, doi:10.1029/97jd02243, 1997.

686 Johnson, C. E., Bellouin, N., Davison, P. S., Jones, A., Rae, J. G. L., Roberts, D. L., Woodage, M. J., Woodward, S., Or
687 Nez, C. and Savage, N. H.: CLASSIC Aerosol Scheme, Unified Model Doc. Pap. (Vn 10.3) [online] Available from:
688 https://code.metoffice.gov.uk/doc/um/vn10.3/papers/umdp_020.pdf (Accessed 9 March 2017a), 2015.

689 Johnson, J. S., Cui, Z., Lee, L. A., Gosling, J. P., Blyth, A. M. and Carslaw, K. S.: Evaluating uncertainty in convective cloud
690 microphysics using statistical emulation, *J. Adv. Model. Earth Syst.*, 7(1), 162–187, doi:10.1002/2014MS000383,
691 2015b.

692 Kanji, Z. A., Ladino, L. A., Wex, H., Boose, Y., Burkert-Kohn, M., Cziczo, D. J., Krämer, M., Kanji, Z. A., Ladino, L. A., Wex,
693 H., Boose, Y., Burkert-Kohn, M., Cziczo, D. J. and Krämer, M.: Overview of Ice Nucleating Particles, *Meteorol. Monogr.*,
694 58, 1.1-1.33, doi:10.1175/AMSMONOGRAPHS-D-16-0006.1, 2017.

695 Lacher, L., Steinbacher, M., Bukowiecki, N., Herrmann, E., Zipori, A. and Kanji, Z. A.: Impact of air mass conditions and
696 aerosol properties on ice nucleating particle concentrations at the High Altitude Research Station Jungfraujoch,
697 *Atmosphere (Basel)*, 9(9), 363, doi:10.3390/atmos9090363, 2018.

698 Ladino, L. A., Korolev, A., Heckman, I., Wolde, M., Fridlind, A. M. and Ackerman, A. S.: On the role of ice-nucleating
699 aerosol in the formation of ice particles in tropical mesoscale convective systems, *Geophys. Res. Lett.*, 44(3), 1574–
700 1582, doi:10.1002/2016GL072455, 2017.

701 Lasher-Trapp, S., Leon, D. C., DeMott, P. J., Villanueva-Birriel, C. M., Johnson, A. V., Moser, D. H., Tully, C. S. and Wu,
702 W.: A Multisensor Investigation of Rime Splintering in Tropical Maritime Cumuli, *J. Atmos. Sci.*, 73(6), 2547–2564,
703 doi:10.1175/JAS-D-15-0285.1, 2016.

704 Lauber, A., Kiselev, A., Pander, T., Handmann, P., Leisner, T., Lauber, A., Kiselev, A., Pander, T., Handmann, P. and
705 Leisner, T.: Secondary Ice Formation during Freezing of Levitated Droplets, *J. Atmos. Sci.*, 75(8), 2815–2826,

706 doi:10.1175/JAS-D-18-0052.1, 2018.

707 Lawson, R. P., Woods, S., Morrison, H., Lawson, R. P., Woods, S. and Morrison, H.: The Microphysics of Ice and
708 Precipitation Development in Tropical Cumulus Clouds, *J. Atmos. Sci.*, 72(6), 2429–2445, doi:10.1175/JAS-D-14-0274.1,
709 2015.

710 Liu, X., Fu, Y., Cao, Z. and Jin, S.: Influence of ice nuclei parameterization schemes on the hail process, *Adv. Meteorol.*,
711 2018, doi:10.1155/2018/4204137, 2018.

712 Lloyd, G., Choulaton, T., Bower, K., Crosier, J., Gallagher, M., Flynn, M., Dorsey, J., Liu, D., Taylor, J. W., Schlenker, O.,
713 Fugal, J., Borrmann, S., Cotton, R., Field, P. and Blyth, A.: Small Ice Particles at Slightly Supercooled Temperatures in
714 Tropical Maritime Convection, *Atmos. Chem. Phys. Discuss.*, 1–18, doi:10.5194/acp-2019-345, 2019.

715 Lohmann, U., Lüönd, F. and Mahrt, F.: An introduction to clouds: From the microscale to climate, Cambridge
716 University Press., 2016.

717 Luo, Z. and Rossow, W. B.: Characterizing tropical cirrus life cycle, evolution, and interaction with upper-tropospheric
718 water vapor using lagrangian trajectory analysis of satellite observations, *J. Clim.*, 17(23), 4541–4563,
719 doi:10.1175/3222.1, 2004.

720 Mace, G. G., Deng, M., Soden, B. and Zipser, E.: Association of tropical cirrus in the 10–15-km layer with deep
721 convective sources: An observational study combining millimeter radar data and satellite-derived trajectories, *J.*
722 *Atmos. Sci.*, 63(2), 480–503, doi:10.1175/JAS3627.1, 2006.

723 Manners, J., Edwards, J. M., Hill, P. and Thelen, J.-C.: SOCRATES technical guide Suite Of Community Radiative Transfer
724 codes based on Edwards and Slingo., 2017.

725 McCoy, D. T., Field, P. R., Schmidt, A., Grosvenor, D. P., A-M Bender, F., Shipway, B. J., Hill, A. A., Wilkinson, J. M. and
726 Elsaesser, G. S.: Aerosol midlatitude cyclone indirect effects in observations and high-resolution simulations, *Atmos.*
727 *Chem. Phys.*, 18, 5821–5846, doi:10.5194/acp-18-5821-2018, 2018.

728 Meyers, M. P., DeMott, P. J., Cotton, W. R., Meyers, M. P., DeMott, P. J. and Cotton, W. R.: New primary ice-nucleation
729 parameterizations in an explicit cloud model, *J. Appl. Meteorol.*, 31(7), 708–721, doi:10.1175/1520-
730 0450(1992)031<0708:NPINPI>2.0.CO;2, 1992.

731 Miltenberger, A. K., Field, P. R., Hill, A. A., Rosenberg, P., Shipway, B. J., Wilkinson, J. M., Scovell, R. and Blyth, A. M.:
732 Aerosol–cloud interactions in mixed-phase convective clouds – Part 1: Aerosol perturbations, *Atmos. Chem. Phys.*,
733 18(5), 3119–3145, doi:10.5194/acp-18-3119-2018, 2018.

734 Mossop, S. C.: Secondary ice particle production during rime growth: The effect of drop size distribution and rimer
735 velocity, *Q. J. R. Meteorol. Soc.*, 111(470), 1113–1124, doi:10.1002/qj.49711147012, 1985.

736 Niemand, M., Möhler, O., Vogel, B., Vogel, H., Hoose, C., Connolly, P., Klein, H., Bingemer, H., DeMott, P., Skrotzki, J.,
737 Leisner, T., Niemand, M., Möhler, O., Vogel, B., Vogel, H., Hoose, C., Connolly, P., Klein, H., Bingemer, H., DeMott, P.,
738 Skrotzki, J. and Leisner, T.: A particle-surface-area-based parameterization of immersion freezing on desert dust
739 particles, *J. Atmos. Sci.*, 69(10), 3077–3092, doi:10.1175/JAS-D-11-0249.1, 2012.

740 O’Sullivan, D., Adams, M. P., Tarn, M. D., Harrison, A. D., Vergara-Temprado, J., Porter, G. C. E., Holden, M. A.,

741 Sanchez-Marroquin, A., Carotenuto, F., Whale, T. F., McQuaid, J. B., Walshaw, R., Hedges, D. H. P., Burke, I. T., Cui, Z.
742 and Murray, B. J.: Contributions of biogenic material to the atmospheric ice-nucleating particle population in North
743 Western Europe, *Sci. Rep.*, 8(1), doi:10.1038/s41598-018-31981-7, 2018.

744 Peckhaus, A., Kiselev, A., Hiron, T., Ebert, M. and Leisner, T.: A comparative study of K-rich and Na/Ca-rich feldspar ice-
745 nucleating particles in a nanoliter droplet freezing assay, *Atmos. Chem. Phys.*, 16(18), 11477–11496, doi:10.5194/acp-
746 16-11477-2016, 2016.

747 Phillips, V. T. J., Andronache, C., Sherwood, S. C., Bansemer, A., Conant, W. C., Demott, P. J., Flagan, R. C., Heymsfield,
748 A., Jonsson, H., Poellot, M., Rissman, T. A., Seinfeld, J. H., Vanreken, T., Varutbangkul, V. and Wilson, J. C.: Anvil
749 glaciation in a deep cumulus updraught over Florida simulated with the Explicit Microphysics Model. I: Impact of
750 various nucleation processes, *Q. J. R. Meteorol. Soc.*, 131(609), 2019–2046, doi:10.1256/qj.04.85, 2005.

751 Phillips, V. T. J., Donner, L. J., Garner, S. T., Phillips, V. T. J., Donner, L. J. and Garner, S. T.: Nucleation processes in deep
752 convection simulated by a cloud-system-resolving model with double-moment bulk microphysics, *J. Atmos. Sci.*, 64(3),
753 738–761, doi:10.1175/JAS3869.1, 2007.

754 Phillips, V. T. J., Patade, S., Gutierrez, J. and Bansemer, A.: Secondary Ice Production by Fragmentation of Freezing
755 Drops: Formulation and Theory, *J. Atmos. Sci.*, 75, 3031–3070, doi:10.1175/JAS-D-17-0190.1, 2018.

756 Price, H. C., Baustian, K. J., McQuaid, J. B., Blyth, A., Bower, K. N., Choullarton, T., Cotton, R. J., Cui, Z., Field, P. R.,
757 Gallagher, M., Hawker, R., Merrington, A., Miltenberger, A., Neely III, R. R., Parker, S. T., Rosenberg, P. D., Taylor, J. W.,
758 Trembath, J., Vergara-Temprado, J., Whale, T. F., Wilson, T. W., Young, G. and Murray, B. J.: Atmospheric ice-
759 nucleating particles in the dusty tropical Atlantic, *J. Geophys. Res. Atmos.*, 123(4), 2175–2193,
760 doi:10.1002/2017JD027560, 2018.

761 Saunders, C. P. . and Hosseini, A. .: A laboratory study of the effect of velocity on Hallett–Mossop ice crystal
762 multiplication, *Atmos. Res.*, 59–60, 3–14, doi:10.1016/S0169-8095(01)00106-5, 2001.

763 Seinfeld, J. H. and Spyros, N. P.: *Atmospheric Chemistry and Physics: From Air Pollution to Climate Change*, 3rd ed.,
764 Wiley, New York, USA. [online] Available from: [https://www.amazon.co.uk/Atmospheric-Chemistry-Physics-Pollution-
765 Climate/dp/0471720186](https://www.amazon.co.uk/Atmospheric-Chemistry-Physics-Pollution-Climate/dp/0471720186) (Accessed 29 October 2019), 2006.

766 Shi, Y. and Liu, X.: Dust Radiative Effects on Climate by Glaciating Mixed-Phase Clouds, *Geophys. Res. Lett.*, 46(11),
767 6128–6137, doi:10.1029/2019GL082504, 2019.

768 Stevens, R. G., Loewe, K., Dearden, C., Dimitrellos, A., Possner, A., Eirund, G. K., Raatikainen, T., Hill, A. A., Shipway, B.
769 J., Wilkinson, J., Romakkaniemi, S., Tonttila, J., Laaksonen, A., Korhonen, H., Connolly, P., Lohmann, U., Hoose, C.,
770 Ekman, A. M. L., Carslaw, K. S. and Field, P. R.: A model intercomparison of CCN-limited tenuous clouds in the high
771 Arctic, *Atmos. Chem. Phys.*, 18, 11041–11071, doi:10.5194/acp-18-11041-2018, 2018.

772 Sullivan, S. C., Hoose, C., Kiselev, A., Leisner, T. and Nenes, A.: Initiation of secondary ice production in clouds, *Atmos.*
773 *Chem. Phys.*, 18, 1593–1610, doi:10.5194/acp-18-1593-2018, 2018.

774 Takeishi, A. and Storelvmo, T.: A study of enhanced heterogeneous ice nucleation in simulated deep convective clouds
775 observed during DC3, *J. Geophys. Res. Atmos.*, 123(23), 13,396-13,420, doi:10.1029/2018JD028889, 2018.

776 Vali, G., Demott, P. J., Möhler, O. and Whale, T. F.: Technical Note: A proposal for ice nucleation terminology, *Atmos.*

777 Chem. Phys, 15, 10263–10270, doi:10.5194/acp-15-10263-2015, 2015.

778 Vergara-Temprado, J., Murray, B. J., Wilson, T. W., O’sullivan, D., Browse, J., Pringle, K. J., Ardon-Dryer, K., Bertram, A.
779 K., Burrows, S. M., Ceburnis, D., Demott, P. J., Mason, R. H., O’dowd, C. D., Rinaldi, M. and Carslaw, K. S.: Contribution
780 of feldspar and marine organic aerosols to global ice nucleating particle concentrations, Atmos. Chem. Phys, 17, 3637–
781 3658, doi:10.5194/acp-17-3637-2017, 2017.

782 Vergara-Temprado, J., Miltenberger, A. K., Furtado, K., Grosvenor, D. P., Shipway, B. J., Hill, A. A., Wilkinson, J. M.,
783 Field, P. R., Murray, B. J. and Carslaw, K. S.: Strong control of Southern Ocean cloud reflectivity by ice-nucleating
784 particles., Proc. Natl. Acad. Sci. U. S. A., 115(11), 2687–2692, doi:10.1073/pnas.1721627115, 2018.

785 Waliser, D. E., Li, J. L. F., Woods, C. P., Austin, R. T., Bacmeister, J., Chern, J., Del Genio, A., Jiang, J. H., Kuang, Z., Meng,
786 H., Minnis, P., Platnick, S., Rossow, W. B., Stephens, G. L., Sun-Mack, S., Tao, W. K., Tompkins, A. M., Vane, D. G.,
787 Walker, C. and Wu, D.: Cloud ice: A climate model challenge with signs and expectations of progress, J. Geophys. Res.
788 Atmos., 114(8), doi:10.1029/2008JD010015, 2009.

789 Walters, D., Boutle, I., Brooks, M., Melvin, T., Stratton, R., Vosper, S., Wells, H., Williams, K., Wood, N., Allen, T.,
790 Bushell, A., Copey, D., Earnshaw, P., Edwards, J., Gross, M., Hardiman, S., Harris, C., Heming, J., Klingaman, N., Levine,
791 R., Manners, J., Martin, G., Milton, S., Mittermaier, M., Morcrette, C., Riddick, T., Roberts, M., Sanchez, C., Selwood,
792 P., Stirling, A., Smith, C., Suri, D., Tennant, W., Luigi Vidale, P., Wilkinson, J., Willett, M., Woolnough, S. and Xavier, P.:
793 The Met Office Unified Model Global Atmosphere 6.0/6.1 and JULES Global Land 6.0/6.1 configurations, Geosci.
794 Model Dev., 10(4), 1487–1520, doi:10.5194/gmd-10-1487-2017, 2017.

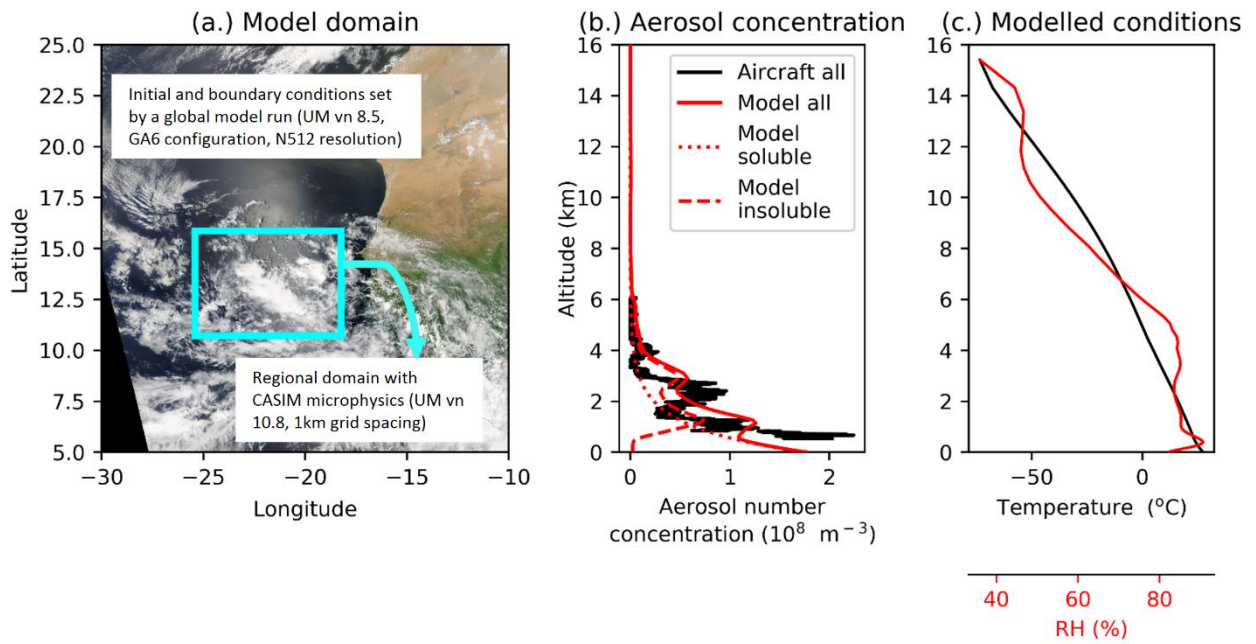
795 Welti, A., Müller, K., Fleming, Z. L. and Stratmann, F.: Concentration and variability of ice nuclei in the subtropical
796 maritime boundary layer, Atmos. Chem. Phys, 18, 5307–5320, doi:10.5194/acp-18-5307-2018, 2018.

797 Wilson, T. W., Ladino, L. A., Alpert, P. A., Breckels, M. N., Brooks, I. M., Browse, J., Burrows, S. M., Carslaw, K. S.,
798 Huffman, J. A., Judd, C., Kilthau, W. P., Mason, R. H., McFiggans, G., Miller, L. A., Nájera, J. J., Polishchuk, E., Rae, S.,
799 Schiller, C. L., Si, M., Temprado, J. V., Whale, T. F., Wong, J. P. S., Wurl, O., Yakobi-Hancock, J. D., Abbatt, J. P. D., Aller,
800 J. Y., Bertram, A. K., Knopf, D. A. and Murray, B. J.: A marine biogenic source of atmospheric ice-nucleating particles,
801 Nature, 525(7568), 234–238, doi:10.1038/nature14986, 2015.

802

803

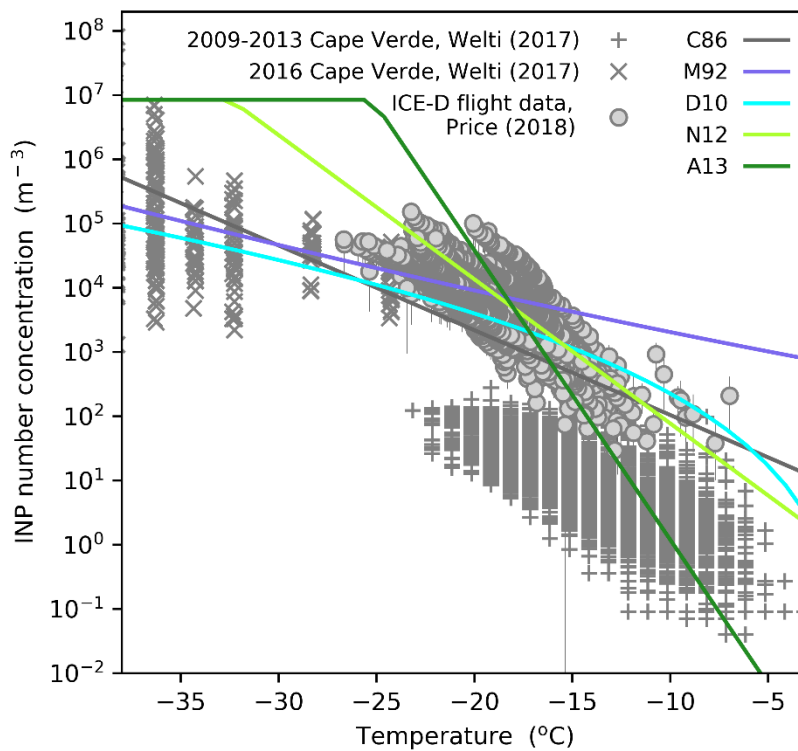
804 **Figures**



805

806 **Figure 1. Modelled domain location and resolution details (a), observed (black line) and modelled (red lines) aerosol**
 807 **concentrations (b), and mean modelled domain mean temperature and relative humidity profiles (c). The observed**
 808 **aerosol profile shown in b was measured using the Passive Cavity Aerosol Spectrometer Probe (PCASP) which captures**
 809 **aerosols between 0.1 and 3µm in size. The insoluble aerosol profile shown in b is extracted from a regional UM vn 10.3**
 810 **simulation (8 km grid spacing, CLASSIC dust scheme). The modelled aerosol profiles are applied throughout the regional**
 811 **domain shown in a at the start of the simulation (00:00 21st August 2015) and at the boundaries throughout. INP**
 812 **concentrations in the D10, N12 and A13 simulations are linked to the insoluble aerosol profile shown in b. The image**
 813 **shown in (a) are moderate resolution imaging spectroradiometer (MODIS) Corrected Reflectance imagery produced using**
 814 **the MODIS Level 1B data and downloaded from the NASA Worldview website.**

815



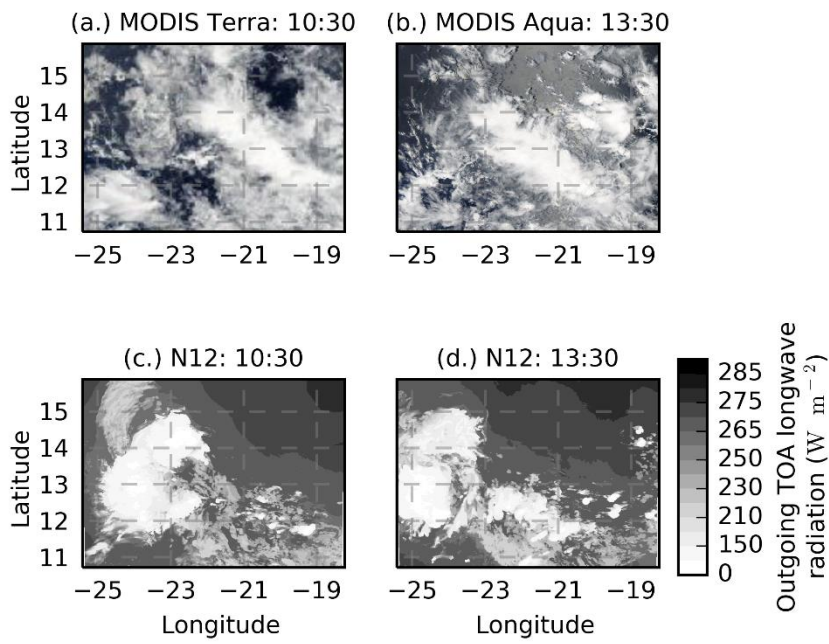
816

817 **Figure 24.** Dependence of INP number concentration on temperature ($d[INP]/dT$) for the five heterogeneous freezing
 818 parameterisations simulated in this study (C86, M92, D10, N12, A13) compared to INP number concentrations measured
 819 in the eastern Tropical Atlantic (Price et al., 2018; Welti et al., 2018). Parameterisations are shown for the aerosol
 820 concentrations at approximately the first freezing level in our simulations ($\sim 8 \text{ cm}^{-3}$). D10, N12 and A13 are dependent on
 821 aerosol concentrations, while C86 and M92 are not dependent on aerosol concentration. For the correlation analysis
 822 where model outputs were plotted against parameterisation slope ($d\log_{10}[INP]/dT$), a straight line was fitted to the
 823 D10 parameterisation between -3 and -37°C to obtain an approximate INP parameterisation slope. Other
 824 temperature ranges were tested and were found to have no notable effect on results.

825

826

827



828

829

830

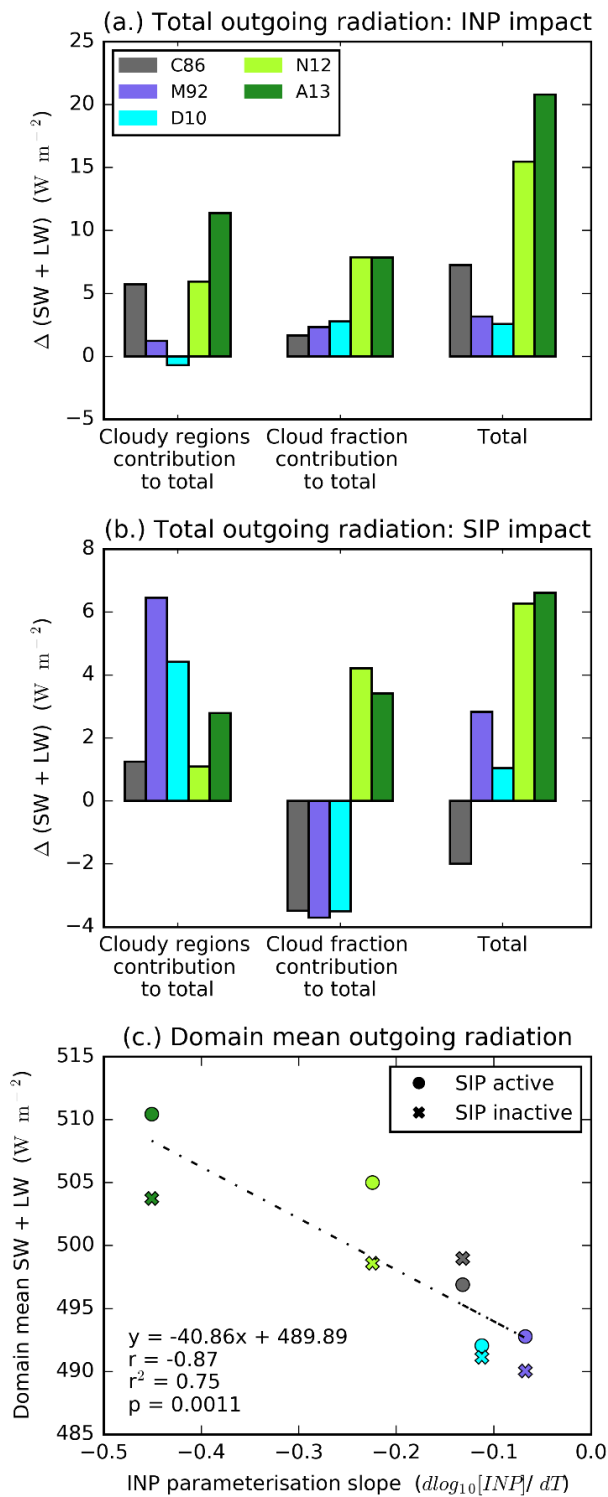
831

832

833

834

Figure 23. Cloud field evolution. MODIS Terra (a) and Aqua (b) corrected reflectance images of the modelled domain for the 21st of August 2015 and the corresponding simulated top of atmosphere outgoing longwave radiation for the N12 simulation ~~throughout the study period (c-h, d)~~. Note that the colour bar relates to panels c and d only. Images shown in (a) and (b) are moderate resolution imaging spectroradiometer (MODIS) Corrected Reflectance imagery produced using the MODIS Level 1B data and downloaded from the NASA Worldview website.



835

836

837

838

839

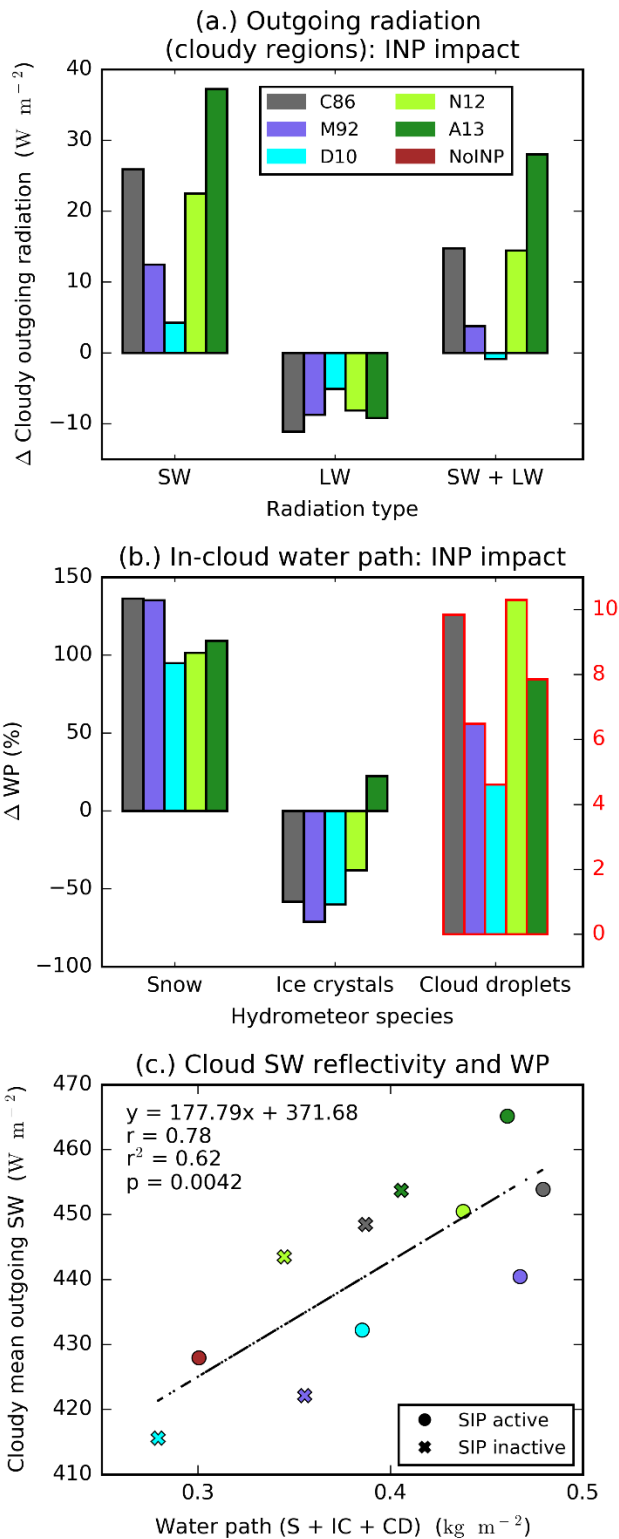
840

841

842

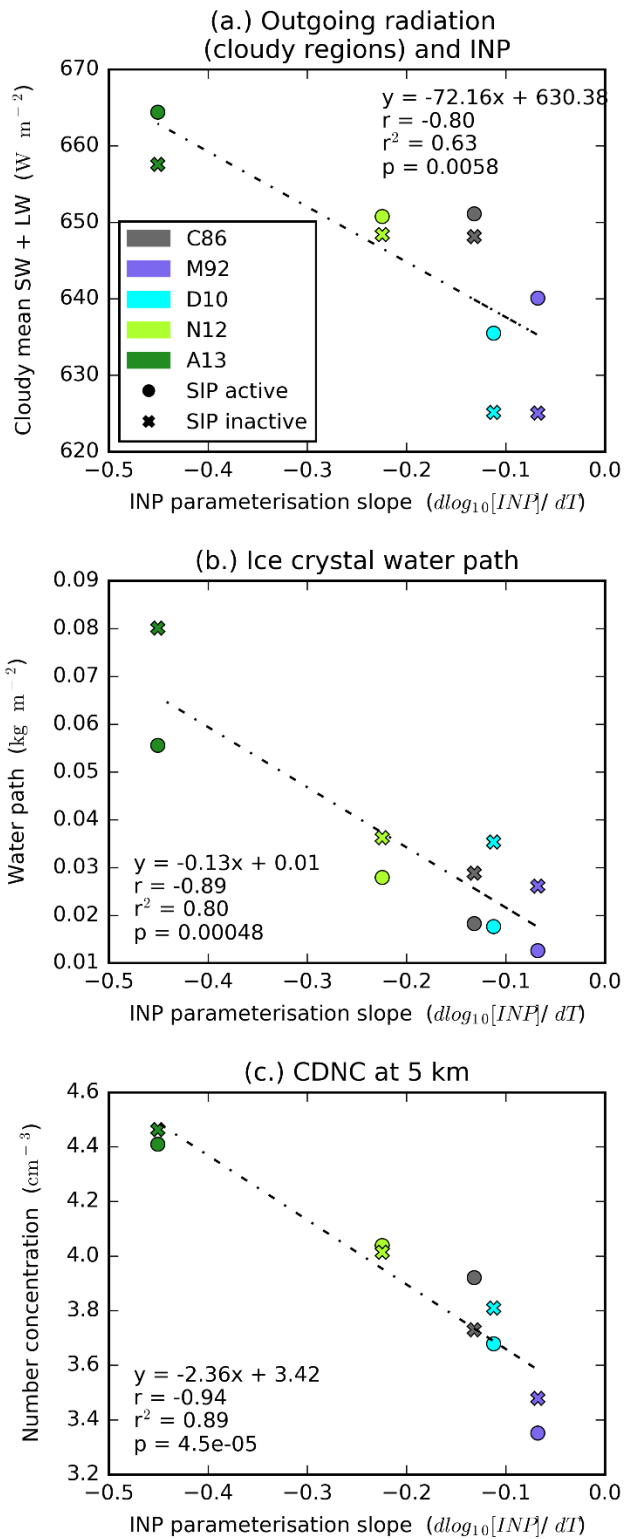
843

Figure 43. Effect of INP and secondary production on top of atmosphere (TOA) outgoing radiation. Effect of INP parameterisation (a) and SIP (a representation of the Hallett Mossop process) (b) on domain-mean daytime TOA outgoing radiation and total domain-mean daytime TOA outgoing radiation plotted against INP parameterisation slope (c). In (a), the change from the NoINP simulation is shown (INP - NoINP) with SIP active. In (b), the change from SIP_active to SIP_inactive is shown (SIP_active – SIP_inactive). A positive value indicates more outgoing radiation when INP or SIP are active. In (a) and (b), the relative contributions of changes in outgoing radiation from cloudy regions (left) and cloud fraction (middle) to the total radiative forcing (right) are shown (calculation described in Sect. 2.1.3). In addition to the simulated values, a regression line (n=10) is shown in (c) along with its associated statistical descriptors.



844
845

846 **Figure 54.** INP and outgoing radiation from cloudy regions. Absolute change in outgoing shortwave, longwave and total
 847 radiation from cloudy regions relative to the NoINP simulation (a), the percentage change in water path (WP) associated
 848 with snow (S), ice crystals (IC) and cloud droplets (CD) relative to the NoINP simulation (b), and mean daytime outgoing
 849 shortwave from cloudy regions plotted against the sum of S, IC and CD water paths (c). Note different scale for CD water
 850 path in (b). In addition to the simulated values, a regression line (n=11) is shown in (c) along with its associated statistical
 851 descriptors.



852

853

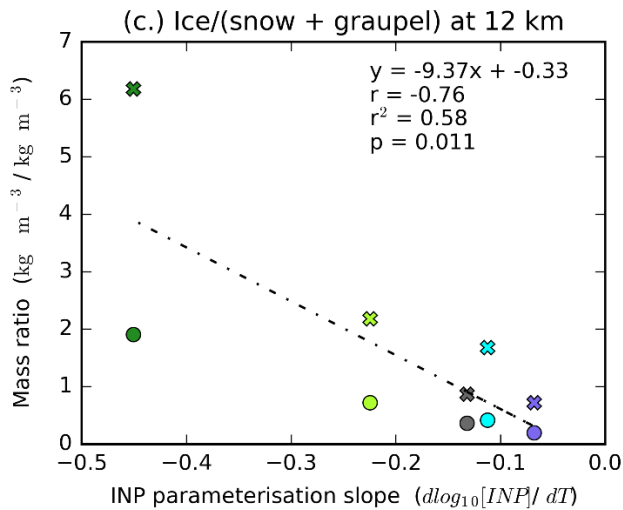
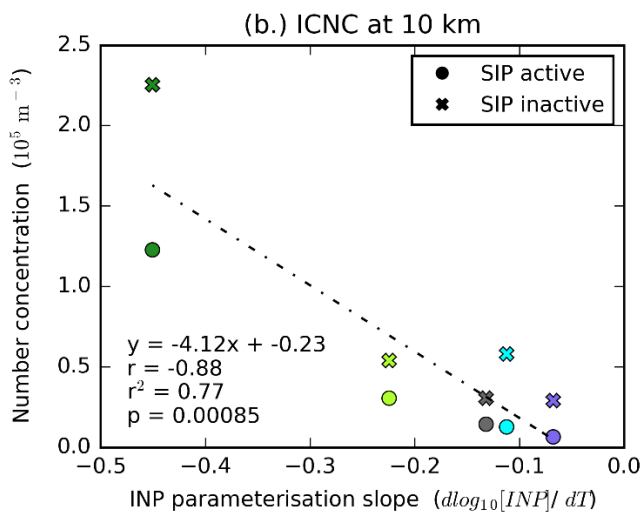
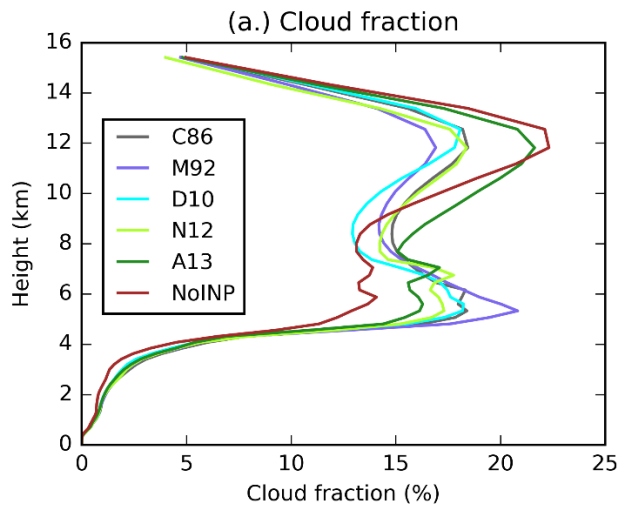
854

855

856

857

Figure 65. Outgoing radiation from cloudy regions and INP parameterisation slope. Scatter plots of INP parameterisation slope and total daytime outgoing radiation from cloudy regions (a), in-cloud mean ice crystal (cloud ice only) water path (b), and in-cloud cloud droplet number concentrations at the start of the mixed-phase region (5 km) (c). Also shown are the respective regression lines (n=10) and associated statistical descriptors.



858

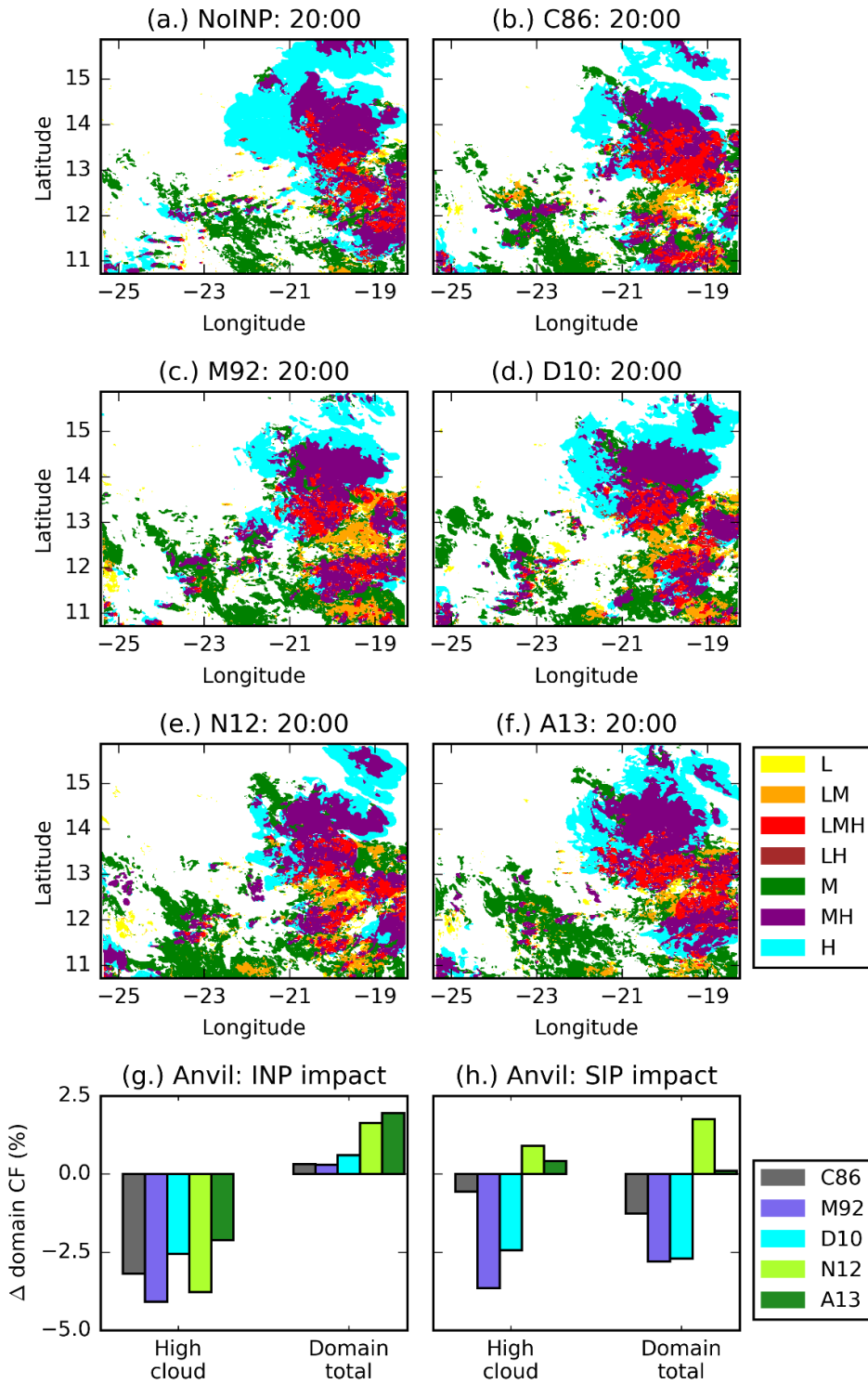
859

860

861

862

Figure 76. Cloud fraction and INP parameterisation slope. Domain-mean cloud fraction profile (a), INP parameterisation slope plotted against ice crystal number concentration at 10 km (b) and mass ratio of ice crystals to snow plus graupel at 12 km (c). Also shown in (b) and (c) are the respective regression lines (n=10) and associated statistical descriptors.



863

864

865

866

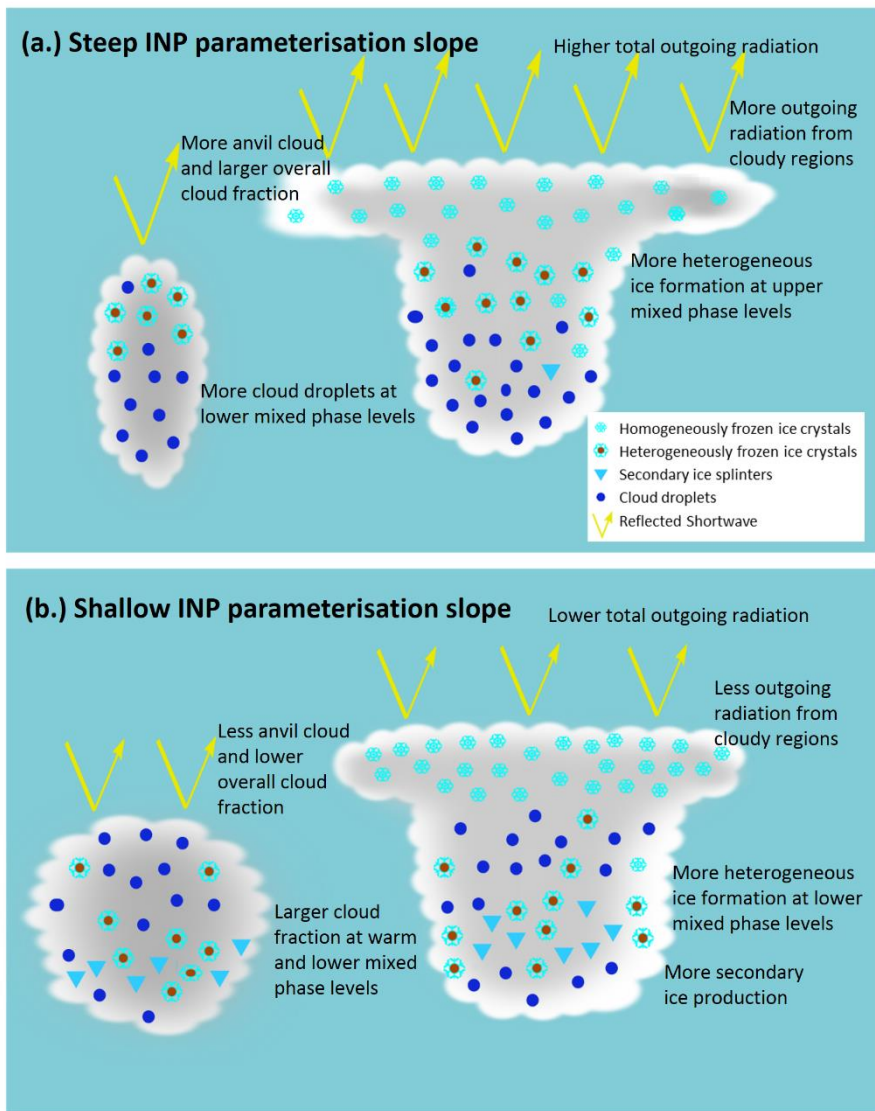
867

868

869

870

Figure 87. Vertical composition of cloud. 2D distribution of cloud type at 20:00 for all six SIP_active simulations (a-f), as well as anvil and domain cloud fraction change due to INP (g) and due to SIP (h). Clouds are categorised according to their altitude into low (L, <4 km), mid (M, 4-9 km) and high (H, >9 km) levels and mixed category columns if cloud (containing more than 10^{-5} kg kg^{-1} condensed water from cloud droplets, ice crystals, snow and graupel) was present in more than one of these levels (a more detailed description can be found in Sect. 2.1.4). A positive value in (g) or (h) indicates higher values when INP (g) or SIP (h) are active.



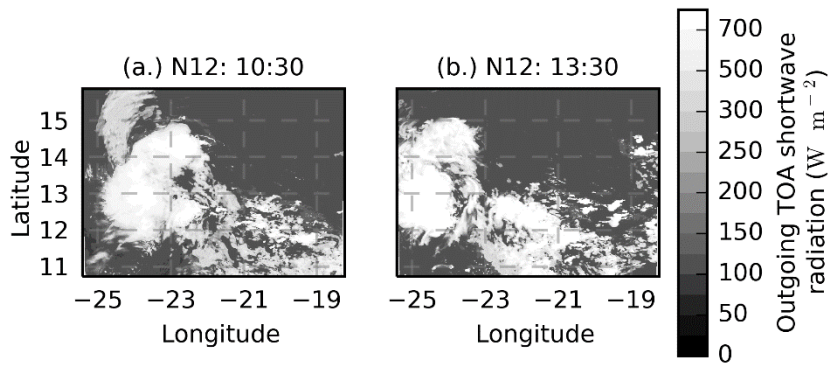
871

872 **Figure 9. Schematic of the main effects of INP parameterisation slope (i.e. a steep (a) or shallow (b) temperature**
 873 **dependence of INP number concentrations).**

874

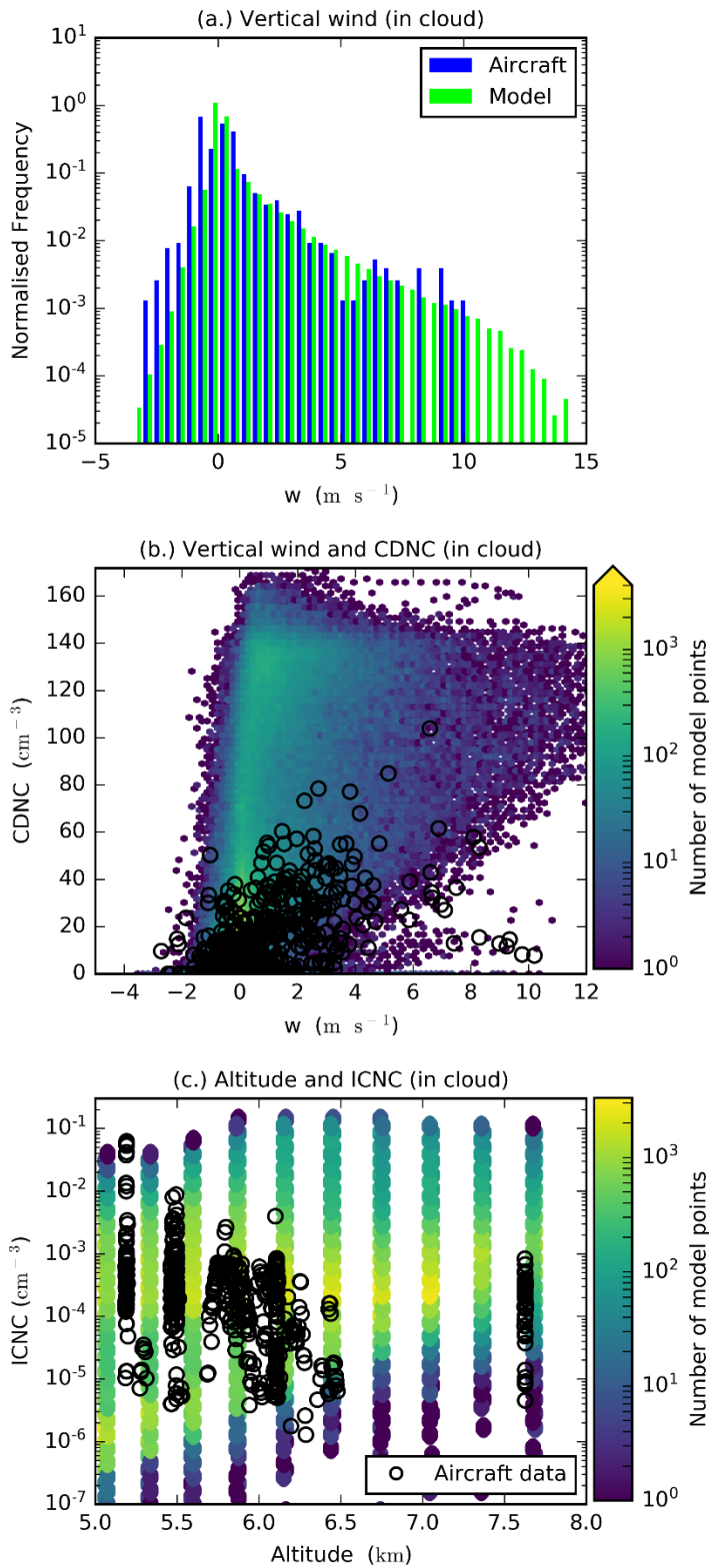
875 **Appendix A**

876



877

878 **Figure A12. The cloud field. Cloud field evolution. Simulated top of atmosphere outgoing shortwave radiation for the N12**
879 **simulation at 10:30 (a) and 13:30 (b) in the daylight hours throughout the study period (a-f).**



880

881

882

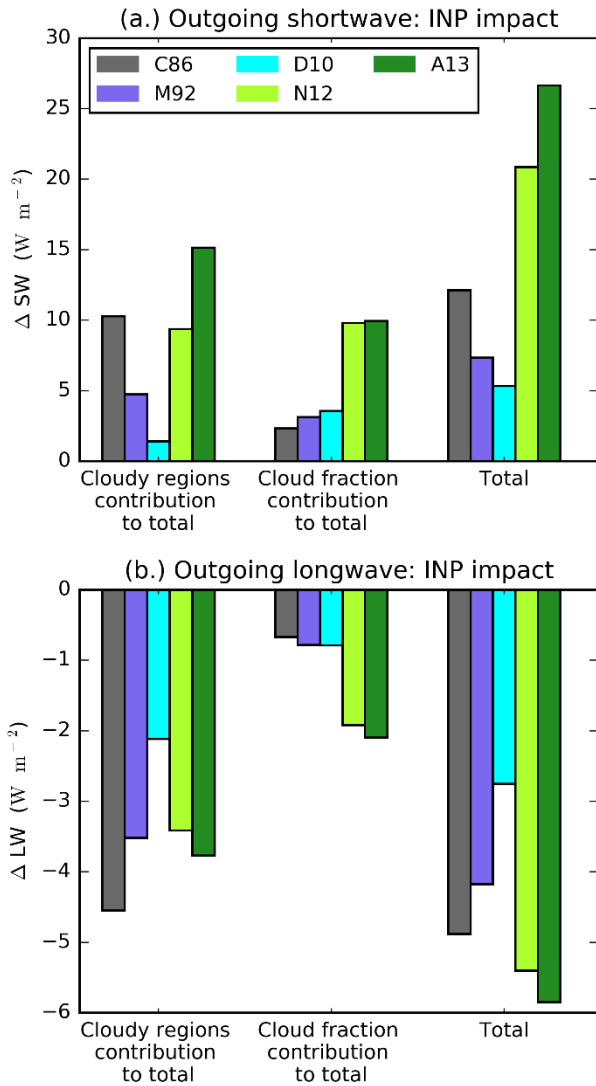
883

884

885

886

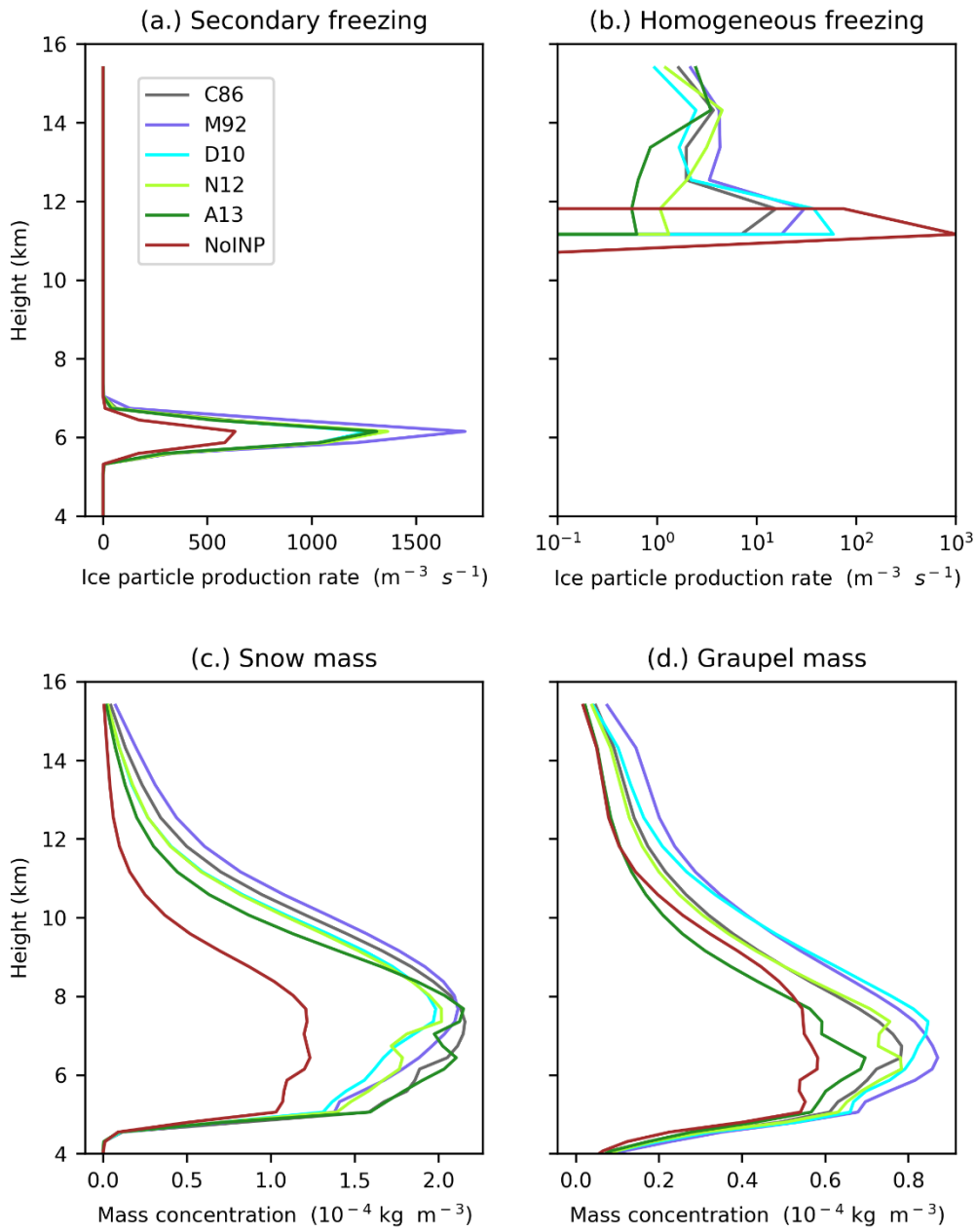
Figure A32. Comparison of observed conditions from the b933 ICED field campaign flight on the 21st August 2015 and the modelled conditions. Vertical wind speed from the model and aircraft data (a), a 2D histograms of modelled vertical wind against cloud droplet number concentration (CDNC) (b) and altitude plotted against ice crystal number concentration (ICNC) (c) with the aircraft data overlaid. Modelled values are selected from clouds between 10 and 150 km^2 in size from the N12 simulation.



888

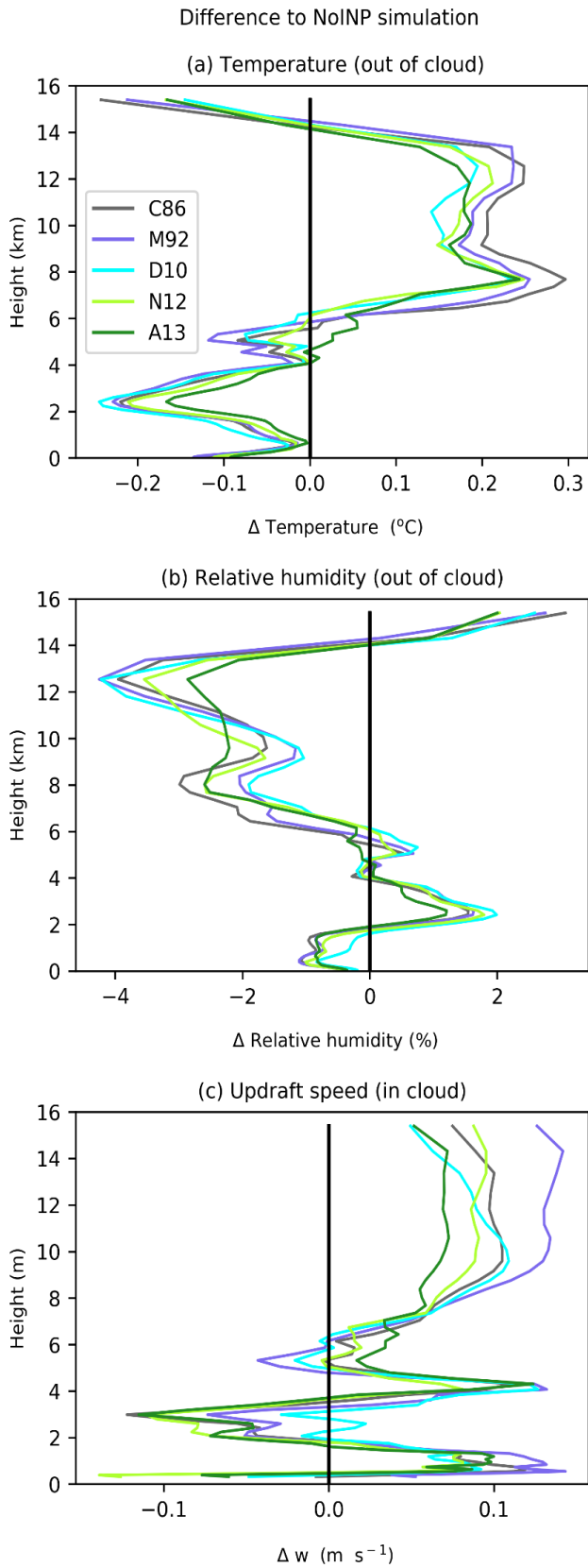
889 **Figure A43.** Effect of INP on domain mean daytime outgoing TOA shortwave and longwave radiation. The change from the
 890 NoINP simulation is shown (INP - NoINP). A positive value indicates more outgoing radiation when INP are present. The
 891 contributions of changes in outgoing radiation from cloudy regions (left) and cloud fraction (middle) to the total radiative
 892 forcing (right) are also shown.

893



894

895 **Figure A54.** Profiles of some microphysical properties of the simulated clouds. Mean in-cloud ice particle production rates
 896 from secondary (b) and homogeneous (c) freezing, snow mass concentration (c) and graupel mass concentration (d).
 897



899

900

901

902

Figure A65. Effect of INP on domain mean out of cloud temperature (a) and relative humidity (b), and in cloud updraft speed (c). The difference from the NoINP simulation is shown, a positive value indicates a higher value when INP is present.